Beihang University
Université Libre de Bruxelles

Search for new physics in dilepton final states at the CMS experiment

Wenxing Fang

Thesis submitted for the degree of

Doctor of Philosophy

Bruxelles, 13 June 2019

Defense date:

– Private: 23th May at Beihang University, Beijing (China)
– Public: 19th June at Université Libre de Bruxelles, Brussels (Belgium)

Doctoral jury:

– Prof. Barbara CLERBAUX (Université Libre de Bruxelles, Belgium), co-promoter
– Prof. Chengping SHEN (Fudan University, China), co-promoter
– Prof. Laura LOPEZ HONOREZ (Université Libre de Bruxelles, Belgium), Chair
– Prof. Li YUAN (Beihang University, China), Secretary
– Prof. Yajun MAO (Peking University, China)
– Dr. Andrea GIAMMANCO (UCL, Belgium)
– Dr. Reza GOLDOUZIAN (University of Notre Dame, USA)

Internal Chinese readers:

– Prof. Yujie ZHANG (Beihang University, China)
– Prof. Huaxing CHEN (Beihang University, China)
– Prof. Yong BAN (Peking University, China)
– Prof. Mingshui CHEN (IHEP, China)
– Prof. Chunxu YU (Nankai University, China)

摘要

该论文介绍了利用双电子末态寻找新的重共振态和在顶夸克产生过程寻找新物理的研究。论文的第一章介绍了粒子物理中的标准模型。紧接着在第二章介绍了一些与研究相关的超标准模型。在第三章介绍了欧洲大型强子对撞机（the Large Hadron Collider，简称 LHC）和紧凑缪子线圈探测器（the Compact Muon Solenoid，简称 CMS）。在随后的一章介绍了 CMS 中粒子的重建技术和过程。最后给出这两个研究的具体介绍。

第一个研究是在双电子末态寻找重的共振态。这个新的共振态是许多超标准模型所预言的，例如大统一理论（the Grand Unified Theories，简称 GUT）和额外维理论。如果存在这种共振态，那么我们将会在双电子不变质量谱中观察到一个新的质量峰。该研究利用了 CMS 在 2016 年采集到的 35.9 fb^{-1} 和在 2017 年采集到的 41.4 fb^{-1} 的数据。采用了优化的事例选择条件以增加其对信号事例选择效率。该分析的主要本底来自 Drell-Yan 过程，该过程利用蒙特卡洛样本（MC）来模拟。对于次要的顶夸克对和类顶夸克对过程，该分析也采用 MC 来模拟，同时利用数据来对 MC 进行检查。对于喷注（jet）误判为电子的本底，该分析利用 data-driven 的方法来估计该本底的贡献。在观察研究了最终的双电子不变质量谱后发现数据的分布与标准模型的预期相符合，并没有看到新物理存在的迹象。因此，在研究的最后给出了相关的新共振态产生截面乘以衰变分支比的上限和对应的新共振态的质量下限。

第二个研究是利用双电子和双缪子末态在顶夸克产生过程中寻找新物理。由于顶夸克是基本粒子中最重的粒子，其与 Higgs 粒子和 W 玻色子有很强的耦合。因此，顶夸克在许多新物理模型中占有重要地位。该研究利用了 CMS 在 2016 年采集到的 35.9 fb^{-1} 的数据。所研究的过程包括顶夸克对（$\mathrm{t\bar{t}}$ ）产生过程和单个顶夸克伴随一个 W 玻色子产生过程（tW）。同时，由于 $\mathrm{t\bar{t}}$ 和 tW 过程很接近，该研究利用了多变量分析的方法去区分 $\mathrm{t\bar{t}}$ 和 tW 过程。由于最终的数据分布和标准模型预期的分布一致，因此并没有发现新物理。最终该研究利用有效场理论给出了对可能存在的新耦合的强度的限制。

关键词: 新物理，双电子，双缪子，重共振态，顶夸克，CMS实验，有效场理论，多变量分析

Résumé

Cette thèse décrit la recherche de nouvelles résonances massives qui se désintègrent en une paires d'électrons et la recherche de nouvelle physique dans le secteur des quarks top. Le modèle standard des particules élémentaires est présentédans le premier chapitre. Ensuite, nous décrivons une sélection de théories au-delàdu modèle standard prédisant l'existence de nouvelles résonances massives, ainsi qu'une introduction à la théorie effective des champs utilisée pour la recherche de nouvelles physiques dans le secteur des quark top. Après cela, le collisionneur LHC (Large Hadron Collider) et le détecteur CMS (Compact Muon Solenoid) sont introduits, et les techniques utilisées afin de reconstruire les particules produit dans les collisions sont discutées ensuite. Finalement, deux analyses séparées sont présentées.

La première est la recherche de nouvelles résonances massives dans l'état final diélectron. Certaines théories au-delàdu modèle standard prédisent l'existence de nouvelles résonances massives pouvant se désintégrer en paires d'électrons, telles que les théories de grande unification et les théories qui introduisent des dimensions spatiales supplémentaires. L'observation d'un excès local d'événements dans le spectre de masse invariante diélectron serait la preuve de l'existence d'une nouvelle résonance massive. Les données utilisées proviennent de l'expérience CMS, et correspondent à 35.9 fb^{-1} collectés en 2016 et 41.4 fb^{-1} en 2017. La sélection d'événements est optimisée pour les électrons de haute énergie et pour éviter de perdre des événements de signal potentiels. Le processus principal est le processus Drell-Yan et il est estiméà partir de simulations. Les processus $t\bar{t}$ et $t\bar{t}$-like sont aussi important, et sont également estimés à partir de simulations. La simulation de ce bruit de fond est validée par une méthode d'analyse de données. Le dernier bruit de fond, à savoir les processus de chromodynamique quantique, est déterminé à partir des données. Après inspection du spectre de masse invariante diélectron, aucun excès significatif par rapport au bruit de fond du modèle standard n'est observé, et une limite supérieure à 95% de niveau de confiance est posée sur le rapport entre d'une part le produit de la section efficace de production d'une nouvelle résonance par son rapport de branchement en diélectron, et d'autre part ce même produit mesuréau pic du boson Z.

La deuxième analyse est la recherche de nouvelle physique dans le secteur des quarks top avec les états finaux diélectron et dimuon en utilisant les données collectées par l'expérience CMS en 2016 avec 35.9 fb^{-1}. En raison de sa masse élevée et de sa masse proche de l'énergie de brisure de la symétrie électrofaible, le quark top devrait jouer un rôle important dans plusieurs scénarios de nouvelle physique. Nous recherchons cette nouvelle physique dans la production de paires de quarks top et dans la production d'un seul quark top associéà un boson, et une analyse multivariée est utilisée pour séparer ces deux processus. Aucun écart significatif par rapport aux prédictions du modèle standard n'est observé. Les résultats sont interprétés dans le cadre d'une théorie effective des champs et les contraintes sur les couplages effectifs correspondants sont définies à un niveau de confiance de 95%.

Mots clés: nouvelle physique, diélectron, dimuon, résonances massives, quark top, Expérience CMS, théorie effective des champs, analyse multivariée.

Abstract

This thesis describes searches for new heavy resonances that decay into dielectron final state and searches for new physics in the top quark sector. The standard model of elementary particle is introduced in the first chapter. After that, a selection of theories beyond the standard model that predict the existence of new massive resonances are described together with an introduction to the effective field theory that is used to search for new physics in top quark sector. Then, the Large Hadron Collider (LHC) and the Compact Muon Solenoid (CMS) detector are introduced, and the techniques used in order to reconstruct the particles produced in the collisions are discussed afterwards. Finally, two separate analyses are presented.

The first analysis is searching for new heavy resonances using dielectron final state. As some beyond Standard Model theories predict the existence of new heavy resonances that can decay into dielectron pair, such as the grand unified theories and theories that introduce extra space-like dimensions. An observation of a local "bump" in the dielectron invariant mass spectrum will be an evidence for the existence of a new heavy resonance. The data used is from CMS experiment collected in 2016 with 35.9 fb^{-1} and in 2017 with 41.4 fb^{-1}. The event selection is optimized in order to be highly efficiency for high energy electron and avoid loosing potential signal events. The leading background is the Drell-Yan process and it is estimated from simulation. The sub-leading background is from $\mathrm{t\bar{t}}$ and $\mathrm{t\bar{t}}$-like processes and it is estimated from simulation also. A data-driven method is used to validate the simulation of sub-leading background. The last background from quantum chromodynamics processes is determined by data-driven approach. After having inspected the final dielectron invariant mass spectrum, no significant excess over the standard model background is observed, and upper limit at 95% confidence level is set on the ratio of production cross-section times branching ratio of a new resonance to the one at the Z boson peak.

The second analysis is the search for new physics in the top quark sector with dielectron and dimuon final states using data collected by the CMS experiment in 2016 with 35.9 fb^{-1}. Because of its high mass and close to electroweak symmetry breaking scale, the top quark is expected to play an important role in several new physics scenarios. The new physics in top quark pair production and in single top quark production in association with a W boson are investigated and a dedicated multivariate analysis is used to separate these two processes. No significant deviation from the standard model expectation is observed. Results are interpreted in the framework of an effective field theory and constraints on the relevant effective couplings are set at 95% confidence level.

Key works: new physics, dielectron, dimuon, heavy resonances, top quark, CMS experiment, effective field theory, multivariate analysis.

Acknowledgements

This thesis would have not been possible without the contributions of many people who helped me during the five years of my doctoral studies.

Firstly, I would like to greatly thank Chengping Shen who is my PhD supervisor at Beihang University and supervised the work presented here. We met each other in 2014 for the first time, he was very friendly and enthusiastic. He inspired my interest in particle physics and opened the door to do a PhD thesis. He gave me great guidance, great support, and countless advices during my PhD study in Beihang University. It is him who encouraged and supported me to be a joint PhD between Beihang University and Université Libre de Bruxelles (ULB). Besides, he provided me great help and suggestions when I was searching for a job after my PhD.

Secondly, I would give great thanks to Barbara Clerbaux who is my PhD supervisor at ULB and supervised the work presented here. She is very kind, thoughtful, and supportive. She is expert in CMS and she gave me countless guidance during my PhD study in CMS. When I had some questions, she always can provide me very nice explanations and answers. It is she who leaded me to the world of searching for new physics in CMS. She also cared about my living at Brussels and provided me help without hesitation when I needed.

Then, I want to thank the people with whom I worked in searching for new physics. I want to thank Reza Goldouzian who helped me a lot both in theoretical and experimental parts of my research. Besides, I want to thank Sam Harper for the time he devoted to me in discussions and explanations. I learnt many things in these occasions. A special acknowledgement goes to Xuyang Gao who is one of my best partner of my research, we worked together efficiently and pleasantly. In addition, a great thank goes to Aidan Randle-Conde who helped me a lot at the beginning of my $\mathrm{Z}^{'}$ search study. I would like thank to Laurent Thomas from whom I took over the high $\mathrm{P_T}$ electron selection efficiency study in $\mathrm{Z}^{'}$ searching. I want to thank Giuseppe Fasanella who did a very nice work in the $\mathrm{Z}^{'}$ search team, he is friendly and provided me a very nice Latex template for my PhD thesis.

Moreover, I want to thank the people in IIHE. Firstly, I would like to thank Laurent Favart who is director of IIHE from ULB, we met each other at first time in Beihang University in 2014. He is gentle and friendly as well as taking care of my living in ULB. Secondly, I would thank Pascal Vanlaer who is enthusiastic, easy going and willing to help when I had some questions, he gave me useful comments on my V_{tx} phenomenological study. Then, I want to thank Audrey Terrier who is the secretary at IIHE. She is very kind and helped a lot in my accommodation and living at ULB. Finally, I would like thank to IIHE IT team who works very hard in maintaining and upgrading the IIHE computer cluster which is easy to use and has very high computing efficiency.

A special thank goes to my office mates, Amandeep and Diego, we get alone very well and I wish them all the best for their future.

Last but not least, I would like to thank my family for the great support and understanding during my PhD study.

Although it is impossible to name everyone here, I would like to thank all of you who helped me.

Contents

Summary of the thesis in Chinese 中文概述

该部分简要地概述了本论文中的主要内容。其中包括对标准模型和超标准模型的介绍，同时还介绍了 LHC 和 LHC 上面的四个主要实验。接着着重地介绍了 CMS 探测器的组成和性能。最后分别介绍了利用双电子末态去寻找重的玻色子的研究课题和在顶夸克（top）产生过程寻找新物理的研究课题。

标准模型和超标准模型的介绍

众所周知，标准模型 [1, 2, 3] 是描述基本粒子性质以及粒子间相互作用机制的理论。基本粒子可以分成构成物质的粒子以及传递相互作用的粒子。其中构成物质的基本粒子包括 6 种轻子：电子（e）、电子中微子（ν_e）、缪子（μ）、缪子中微子（ν_μ）、τ 和 τ 中微子（ν_τ），以及 6 种夸克：上夸克（u）、下夸克（d）、粲夸克（c）、奇异夸克（s）、顶夸克（t）和底夸克（b）。所有这些轻子都有相应的反粒子，此外每种夸克还带有有3种颜色量子数（R、G、B）。传递相互作用的粒子包括传递电磁相互作用的光子（γ）、传递强相互作用的胶子（gluon）和传递弱相互作用的 W 玻色子和 Z 玻色子。除了以上的基本粒子外，标准模型中预言的使基本粒子获得质量的希格斯粒子（Higgs）在 2012 年最终被大型强子对撞机（LHC）上的 ATLAS 实验组和 CMS 实验组同时发现 [4, 5]。至此，标准模型中的基本粒子都已被找到，见图1。此外，截止目前粒子物理实验的测量结果都与标准模型的预言相符。因此，标准模型取得了巨大的成功。关于标准模型的更加具体的介绍可以参见第 1 章，该章节还详细的介绍了 Drell-Yan 过程 [6] 和有效场理论（Effective Field Theory，简称 EFT），这是因为它们在本论文的研究中有着重要作用。

虽然标准模型取得了巨大的成功，但是它也存在一些缺陷。例如，在天文学和宇宙学界科学家们通过实验观测的结果普遍认为存在暗物质和暗能量 [7, 8]。其中宇宙中的暗物质占约 25%，暗能量占约 70% 而可见的物质只占约 5%。但是标准模型并未涉及有关暗物质和暗能量的预言，当然也没能提供暗物质和暗能量的候选者。此外，实验上观测到了中微子在传播过程中它的味可以发生变化（例如从 ν_e 到 ν_μ、ν_μ 到 ν_τ 等）即所谓的中微子振荡现象 [9, 10]。中微子振荡现象的存在表明中微子的质量是非零的，这与标准模型中中微子质量为零的假设不相符。众所周知，我们生活在以正物质组成的世界中，那么反物质去哪儿了呢？一般认为在宇宙大爆炸时，正反物质是成对产生的。因此宇宙中应该存在相同的正物质和反物质。标准模型在 Cabibbo-Kobayashi-Maskawa （CMK）矩阵中引入了电荷宇称（CP）破坏的参数，但是该参数远不能解释目前所观测到的正反物质不对称现象。标准模型除了不能很好地解释以上这些现象外，它也存在一些瑕疵。例如，由于标准模型没有考虑引力的相互作用，因此可以假设标准模型直到普朗克能标（10^{19} GeV）都是有效的。但为了得到实验上发现的质量为 125 GeV 的 Higgs 粒子，在标准模型中则需要通过将两个 10^{38} 量级的大数相减得到一个 10^4 量级的数，这在理论上是可以成立的，但看上去非常不自然，这被称做 Higgs 质量 fine-tuning 问题。如果标准模型只到 TeV 能量有效，那么该问题就不存在了。此外，标准模型里存在 19（若加上中微子的 7 个自由参数，则总共为 26 个自

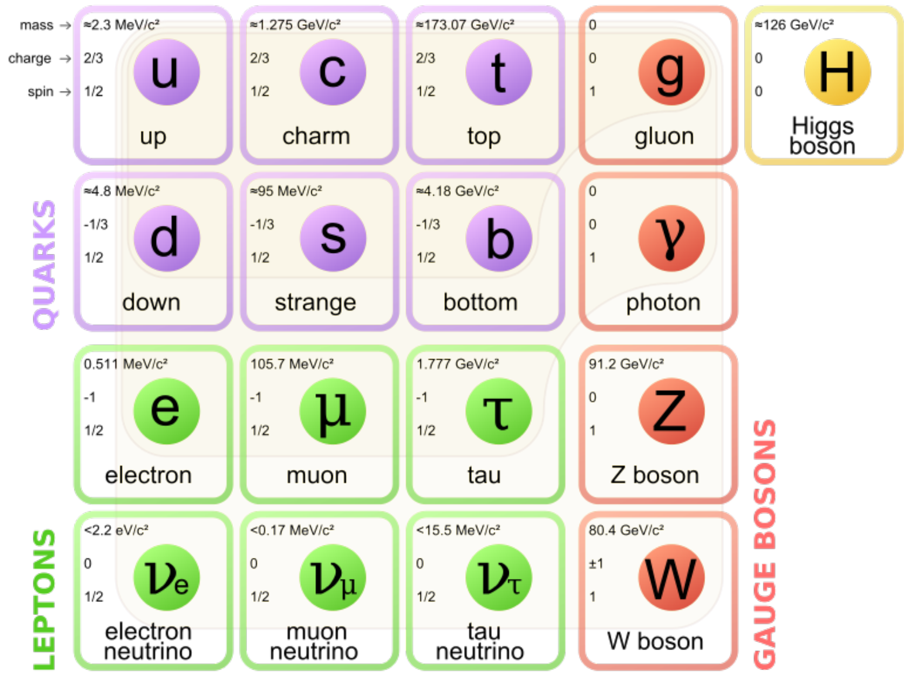

Figure 1: 标准模型中的基本粒子。

由参数）个需要通过实验测量确定的自由参数，这使得它看起来不够简洁。关于标准模型缺陷更加详细的描述可参见 2.1。

正因如此，许多超越标准模型物理学的理论被提了出来。例如超对称模型（SUSY）[11]，在该模型中每一种基本粒子都有一种被称为超对称伙伴（Superpartner）的粒子与之匹配，超对称伙伴的自旋与原粒子相差 1/2 （也就是说玻色子的超对称伙伴是费米子，费米子的超对称伙伴是玻色子），两者质量相同，各种耦合常数间也有着十分明确的关联。这个模型可以很好的消除 Higgs 质量 fine-tuning 的问题以及等级问题（Hierarchy Problem）即为什么在电弱统一能标与大统一或 Planck 能标之间存在高达十几个数量级的差别。同时该模型还为暗物质提供了候选者。此外还有大统一理论（GUT）[12, 13, 14]，该理论想尝试将电磁相互作用、弱相互作用和强相互作用统一起来。对于额外维理论 [15, 16]，该理论想通过引入额外的维度来解释为什么引力的相互作用强度比另外三种相互作用弱 10^{30} 个量级。以上这些超标准模型都预言存在一个新的重玻色子，其可以通过双电子过程衰变。这也是本论文利用双电子末态寻找新的高质量玻色子的动机所在。关于这部分更加详细的介绍可参见 2.2。

如果新物理的能标能在实验中达到，那么新的粒子就能够被产生，可能被直接发现。反之，则需要通过间接的方式去寻找新物理。由于顶夸克是已知基本粒子中最重的粒子以及它与 Higgs 和 W 玻色子都有很强的耦合。因此顶夸克在许多超标准模型中占有很重要的地位。本论文的第二个课题对顶夸克产生过程中可能存在的新物理进行了探索研究。其中包括顶夸克对的产生过程以及单个顶夸克伴随 W 玻色子的产生过程。为了提高该分析对新物理的敏感度，该研究采用了多变量分析方法来区分本底事例和信号事例，同时使用有效场的方法对各种可能存在的新耦合做出与理论模型无关的限制。更多的相关介绍可参见 2.3。

LHC 和 CMS 的介绍

欧洲大型强子对撞机（LHC）是位于法国和瑞士边界，周长为 27 km，位于地下 50 至 150 米之间的质子-质子对撞机，见图 2 的左部分。其质心对撞能量达到了世界最高，在 2015 年到 2018 年该值为 13 TeV。LHC 上主要有四个实验组，见图 2 的右部分。其中包括大型离子对撞器（ALICE）其主要通过铅离子与铅离子对撞或铅离子与质子对撞研究夸克胶子等离子体的性质。还有 LHC 底夸克探测器（LHCb）其主要研究CP破坏、底夸克的性质等。超环面仪器（ATLAS）其是一个综合的粒子探测器，主要研究内容包括精确测量标准模型中的自由参数、寻找 Higgs （在 2012 年已经被发现）、寻找超越标准模型的新物理。紧凑缪子线圈（CMS）其作用与目的和 ATLAS 一致。ATLAS 和 CMS 两个探测器的存在使得各自的实验结果能被互相检查或确认。

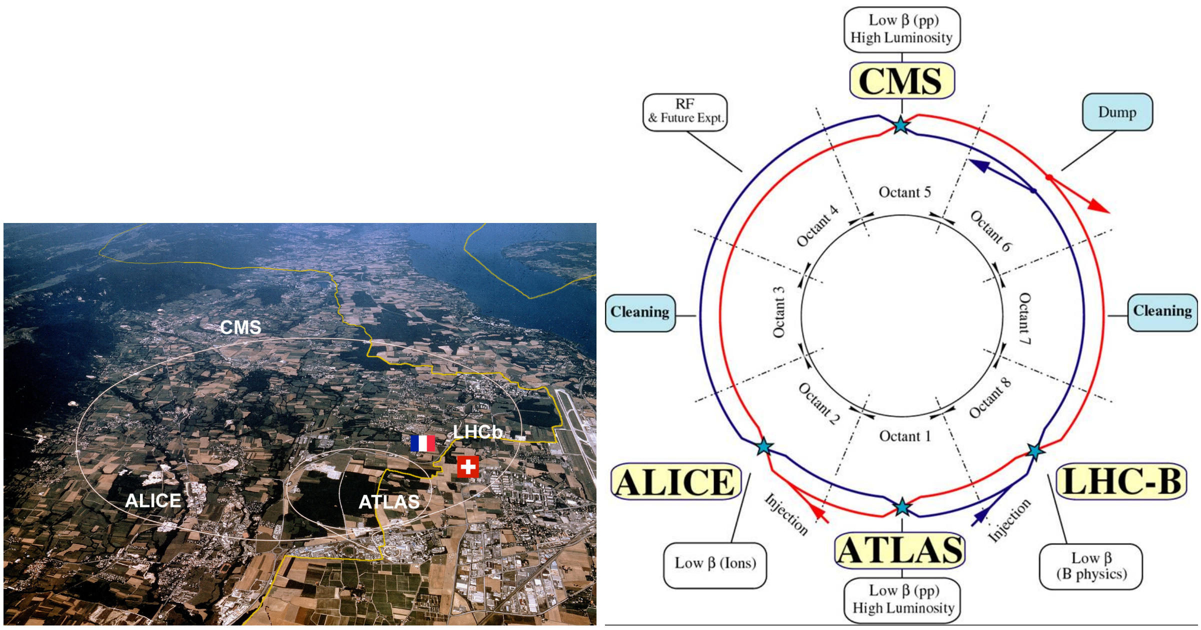

Figure 2: LHC的全貌（左）和LHC 上的四个主要实验（右） [17]。

由于一个质子束团中约有 10^{11} 个质子，因此当质子束团与质子束团发生对撞时，可能产生多个质子-质子对撞顶点，这种现象被称作“pile-up”，“pile-up”现象可见图 3 的左部分，2016 年“pile-up”的分布情况可见图 3 的中间部分以及 2017 年“pile-up”的分布情况可见图 3 的右部分。

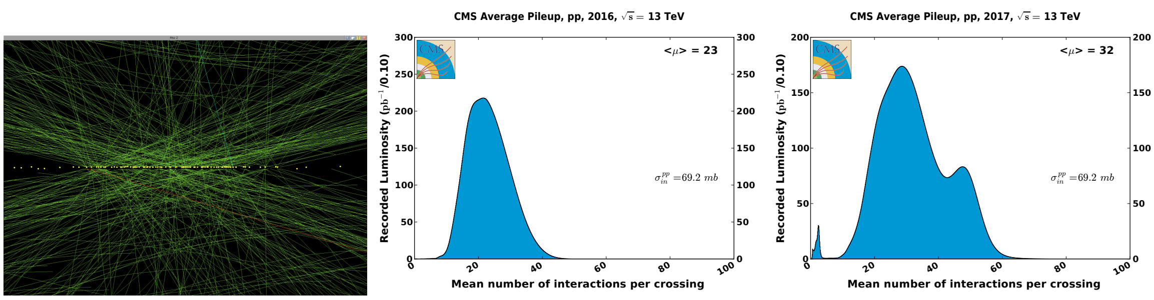

Figure 3: “pile-up”现象（左图），2016 年“pile up”的分布情况（中间）和 2017 年“pile up”的分布情况（右图 [18]。

从 2015 年到 2018 年 LHC 产生了亮度为 156 fb^{-1} 的质子-质子对撞数据，实现了预期的 150 fb^{-1} 目标。在 2024 年以后 LHC 将升级为 HL-LHC 即高亮度 LHC 。关

于 LHC 和 HL-LHC 的取数计划可见图 4。更多的关于 LHC 的介绍可以参见 ??。

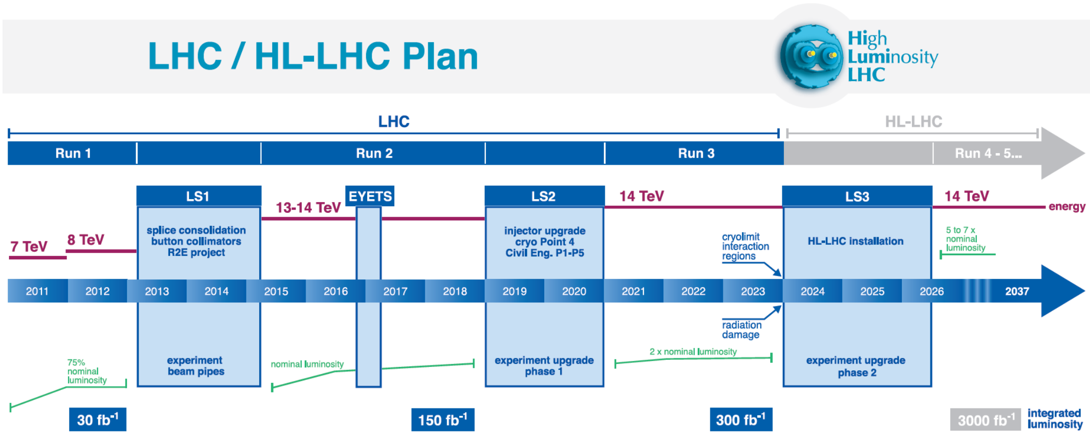

Figure 4: LHC 和 HL-LHC 的取数计划 [19]。

CMS 探测器 [20] 是一个长为 21 米，宽 15 米，高 15 米，重 14000 吨的探测器。从内到外的子探测器依次为硅像素径迹探测器、硅微条径迹探测器、电磁量能器、强子量能器、厄铁线圈以及缪子探测器。CMS 探测器的剖视图和横向截面图可见图 5 和图 6。

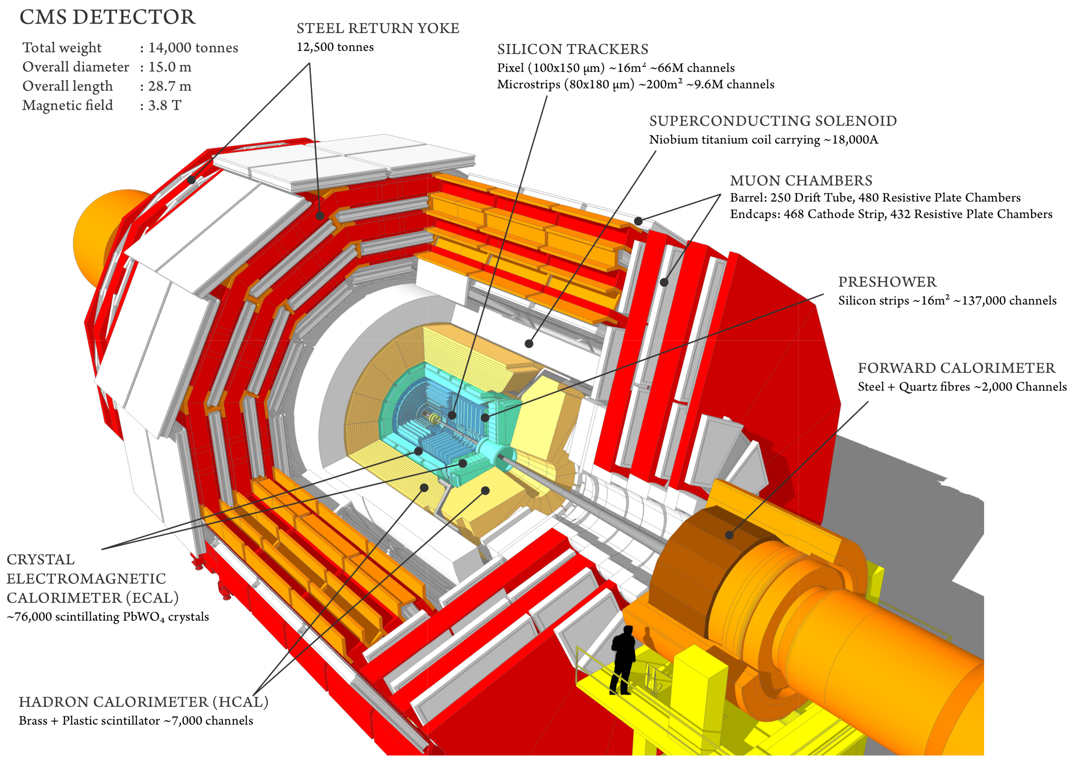

Figure 5: CMS 探测器的剖视图 [21]。

在介绍下面的内容之前有必要先介绍一下 CMS 探测器的坐标系统。CMS 的直角坐标原点为设计时质子-质子对撞的地方，Y 轴的方向向上，X 轴的方向朝向 LHC 的中心，Z 轴的方向朝向 Jura 山脉。X-Y 平面的方位角用 ϕ 表示，与 Z 轴的夹角（即极角）用 θ 表示。CMS 坐标系统定义可见图 7。赝快度 η 的定义为 $\eta = -\ln\tan\theta/2$。横

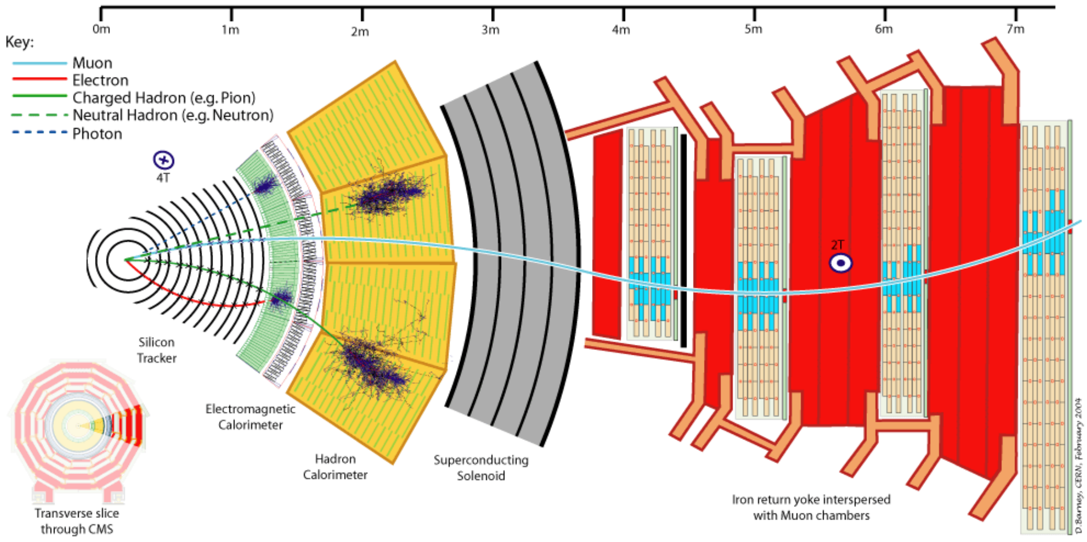

Figure 6: CMS 探测器的横向截面图 [22]。

向动量和横向能量分别用 $\mathrm{p_T}$ 和 $\mathrm{E_T}$ 表示。其中 $\mathrm{p_T(E_T) = p(E)sin\theta}$。在横向面上能量的不平衡值用 $\mathrm{E_T}^{\mathrm{miss}}$ 或$\not{E}_\mathrm{T}$ 表示。其值的计算公式为 $\overrightarrow{\mathrm{E_T}^{\mathrm{miss}}} = -\sum \overrightarrow{\mathrm{E_T}^{\mathrm{exists}}}$。

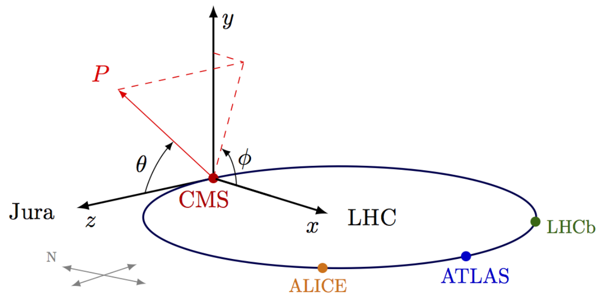

Figure 7: CMS 坐标系统定义。

下面继续介绍 CMS 的各个子探测器。CMS 的硅像素径迹探测器是最靠近输流管的子探测器，其主要目的为探测带电粒子的运动轨迹和质子-质子碰撞的顶点。每个像素的大小为$100 \times 150\ \mu\mathrm{m}^2$，可覆盖 $|\eta|$ 到 2.5 的范围。该探测器设计为能承受瞬时亮度为$1 \times 10^{34}\ \mathrm{cm^{-2}s^{-1}}$，对撞间隔为 25 ns 的质子-质子对撞。硅微条径迹探测器也是为了探测带点粒子的运动轨迹，根据位置的不同其分辨率在 23-52 μm 之间，同样覆盖 $|\eta|$ 到 2.5 的范围。CMS 的硅像素探测器和硅微条探测器组成了 CMS 的径迹探测器。图8 为 CMS 径迹探测器纵向截面图的四分之一，其中黄色部分为 CMS 的硅像素探测器，粉色部分为 CMS 硅微条探测器。

CMS 的电磁量能器的作用是为了测量电子和光子的能量，其由一个桶部（Barrel）和两个端盖（Endcap）组成。桶部由 61200 块（长为 230 mm，宽为 22 mm，高为 22 mm）钨酸铅（$\mathrm{PbWO_4}$ ）晶体组成，可覆盖赝快度从 0 到 1.479。两边端盖部分分别由 7324 块（长为 220 mm，宽为 24.7 mm，高为 24.7 mm）钨酸铅晶体组成，可覆盖 $|\eta|$ 从 1.48 到 3.0 的范围。之所以选择钨酸铅是因为其辐射长度短（$\mathrm{X_0}$ = 0.89 cm）、辐射半径小（2.2 cm）、辐射速度快（80% 的能量在 25 ns 内释放）。为了更好地区分 π^0 和光子，CMS 在每个电磁量能器的端盖前放置了一个 preshower 探测器，覆盖 $|\eta|$ 从 1.65 到 2.6 的范围。图 9 为 CMS 电磁量能器四分之一的纵向截面图。

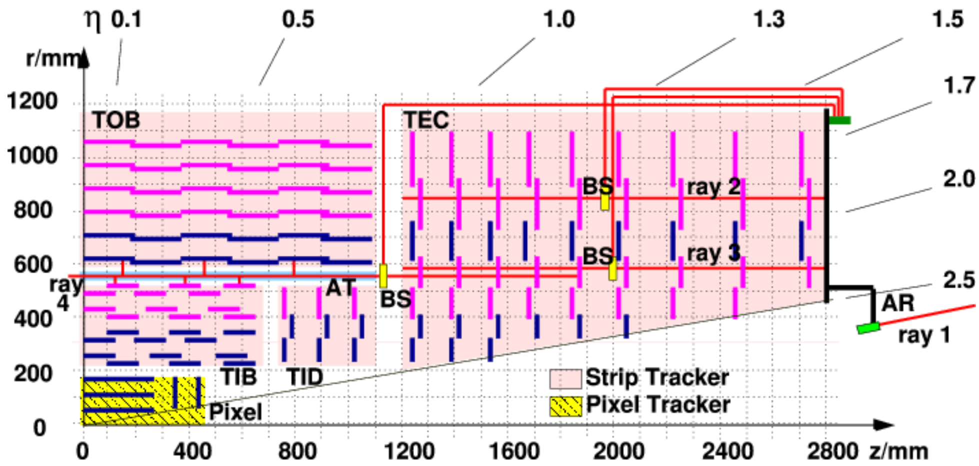

Figure 8: CMS 径迹探测器纵向截面图的四分之一 [20]。

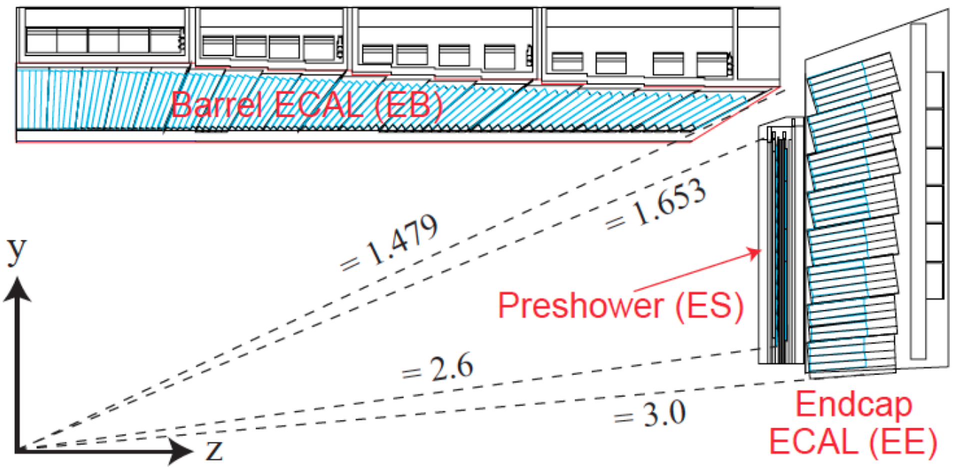

Figure 9: CMS 电磁量能器四分之一的纵向截面图 [23]。

CMS 电磁量能器的能量分辨率可以表示为 [24]:

$$\frac{\sigma}{E}^2 = \frac{S}{\sqrt{E}}^2 + \frac{N}{E}^2 + C^2 \tag{1}$$

其中，S 表示随机项，N 代表噪声项，C 代表常数项。例如对于能量在 20 到 250 GeV 的电子，利用 3×3 的晶体去测量其能量，那么对应的 S 为 0.028 $\sqrt{\text{GeV}}$，N 为 0.12 GeV，C 为 0.003。

在电磁量能器的外面是强子量能器，其目的是测量强子的能量，包括带电的和中性的强子。强子量能器有桶部（HB）、端盖（HE）、前端（HF）和外部（HO）组成。其中 HB 探测范围为 |η| 从 0 到 1.3，HE 探测范围为 |η| 从 1.3 到 3.0，HF 探测范围为 |η| 从 3.0 到 5.2，目的是为了监测质子对撞的瞬时亮度。而 HO 是放在厄铁线圈外的部分，主要是用于对 HB 的辅助测量。关于强子量能器给组成部分在 CMS 探测器中的位置可见图 10。

CMS 强子量能器对单个强子的基准能量分辨率可以表示为 [25]:

$$\frac{\sigma}{E} = \frac{X}{\sqrt{E}} \oplus 5\%, \ \text{X=65\%（HB）, 83\%（HE）, 100\%（HF）} \tag{2}$$

在 CMS 强子量能器外部是 CMS 的厄铁线圈。厄铁线圈利用低温超导技术能提

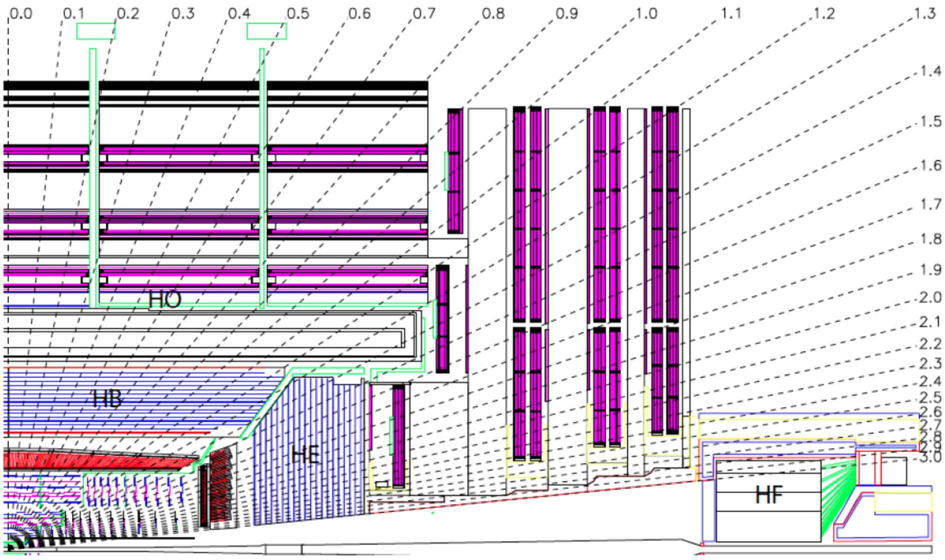

Figure 10: CMS 探测器的纵向截面图。其中分别标明了强子量能器桶部（HB）、端盖（HE）、前端（HF）以及外部（HO）的位置 [20]。

供 3.8 T 的强磁场，使得带电粒子在磁场中运动的轨迹变的弯曲，从而使得带电粒子的动量能被测量。另外厄铁线圈隔绝了几乎所有除了缪子以外的粒子进入其外部的缪子探测器。缪子探测器是 CMS 最外部的子探测器，其主要目的是探测缪子及其动量。缪子探测器由漂移管（DT）、阴极条室（CSC）和阻性板（RPC）组成。其中 DT 和 CSC 提供了很高的缪子空间分辨率，而 RPC 提供了很快的缪子时间分辨率。缪子探测器的桶部（MB）为 $|\eta|$ 从 0 到 1.2 的范围，端盖（ME）的部分为 $|\eta|$ 从 1.2 到 2.4 的范围。图 11 为 CMS 缪子探测器的纵向四分之一截面图。如果只利用缪子探测器的信息，那么对于动量约为 1 TeV的谬子，其动量分辨率在 5% 左右，如果结合 CMS 内部的径迹探测器，那么其动量分辨率可以达到 1% 到 5%。

由于 LHC 质子-质子对撞的频率为 40 MHz（周期为25 ns），每个事例的大小约为 1 MB，而 CMS 数据存储速率上限约为 1 kHz。因此 CMS 利用了两级触发（trigger）来实现对感兴趣事例进行筛选，使得不感兴趣的事例被忽略，而感兴趣的事例能被存储下来。第一级触发被称为 L1 触发，其利用电磁量能器、强子量能器以及谬子探测器来快速判断该事例中是否有能量超过阈值的电子或光子或谬子或中微子或者喷注（jet），为了缩短判断时间 L1 触发并不会使用径迹探测器的信息对光子和电子进行区分。L1 触发的反应时间为 3.2 μs，通过 L1 触发后事例的速率降为约 100 kHz。事例在通过 L1 触发后将会进入第二级 HLT 触发，HLT 将会结合各个子探测器的信息对事例进行重建包括利用径迹探测器来重建带电粒子的径迹。由于需要进行复杂的重建过程，对于每个事例 HLT 将花费约 100 ms 对其是否通过触发进行判断。最终通过 HLT 的事例速率将降为 600 Hz 左右。这些事例将被永久存储到磁盘以用于后续的物理分析。有关 CMS 探测器的介绍和触发可以参见 ??。关于不同粒子的重建过程可以参见 ??。

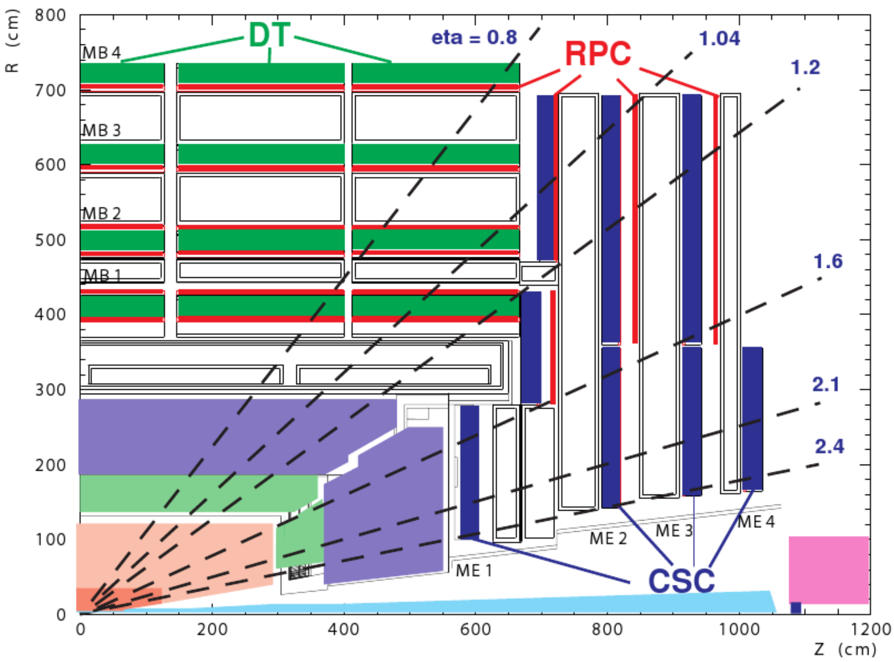

Figure 11: CMS 谬子探测器的纵向四分之一截面图 [20]。

利用双电子末态寻找重的玻色子

在介绍该物理分析之前有必要先介绍一下该物理的总体进展。 LHC 和 Tevatron 在以前就利用过双轻子末态寻找重的玻色子。例如 CMS 利用了 7 TeV [26, 27] 和 8 TeV [28, 29] 以及 2015 年的 13 TeV 加之前 8 TeV [30] 的质子质子对撞数据寻找了 Z' 。最近的 CMS 结果是来自于 2016 年 13 TeV [31] 和 2017 年 13 TeV [32] 的数据，即本论文所要介绍的研究工作。和 CMS 类似， LHC 上的 ATLAS 实验组也做了对 Z' 的寻找。其利用的数据包括： 7 TeV [33, 34]、 8 TeV [35] 和最新的 13 TeV 全部的数据 [36, 37]。在 Tevatron 上， CDF 实验组和 D0 实验组利用 1.96 TeV 的质子和反质子对撞数据对 Z' 进行了寻找 [38, 39, 40, 41, 42, 43]。

本论文的第一个研究课题是利用双电子末态寻找重的玻色子。利用的数据是来自 CMS 的 2016 年 35.9 fb^{-1} 和 2017 年 41.4 fb^{-1} 的数据。对于被选中的电子其必须在电磁量能器的桶部或端盖部分，同时其横向能量要大于 35 GeV，然后通过高能电子选择条件（即 HEEP 选择条件）。我们利用 tag 和 probe 的方法测量了HEEP 的选择效率。其中 tag 为通过 HEEP 条件的电子，并且通过触发表。probe 为普通的电子，此外 tag 和 probe 的不变质量在 Z 玻色子区间。这样做的目的是尽可能减少 probe 中的假电子成分，提高真电子的比例。最后测量到的 HEEP 对真电子的选择效率可见图 12。

对于两个电子都在端盖的事例将不会被选入，因为在高质量区间 QCD 本底对这种事例有较大贡献。最后，被选中的事例需要通过双电子触发表。优化了的事例选择条件能保证对电子具有高的选择效率以及减少非电子被鉴别为电子的误判。该分析的主要本底来源于 Drell-Yan 过程，对于该本底的估计则主要来源于蒙特卡洛（MC）模拟。次主要本底来源于顶夸克对和双玻色子过程，这些本底通过 MC 进行模拟并利用数据对其进行检查。最后一部分的本底来源于 jet 误判为电子的情况，这部分的本底通过 data-driven 的方法进行估计。图 13 为两电子都在端盖时的双电子不变质量谱（左）和质量谱积分（右）在 2016 年（上）和 2017 年（下）。从中可见 data-driven 方法还是能比较好地估计出 jet 本底。

图 14 和 15 分别为来自 2016 年和 2017 年的最终双电子不变质量谱（左）和不变质量谱积分（右）对于两电子都在桶部（上）、一个电子在桶部一个电子在端盖（中）和有一个电子在桶部（下）的情况。可惜在对得到的最终双电子不变质量谱进行研究后并没有发现明显超出标准模型预言的事例。

因此该分析利用统计学的方法给出了不同新粒子产生截面乘以衰变分支比的 95% 的置信上限。同时将该截面乘以衰变分支比上限转换为不同新粒子质量的下限。其结果可见图16。

在结合了双电子道（2016 年 35.9 fb^{-1} 加上 2017 年 41.4 fb^{-1} 的数据）和双缪子道（2016 年 36.3 fb^{-1} 的数据）后，可以给出更严格的不同模型下的 Z' 质量下限，如 Z'_{SSM}（其与标准模型中费米子的耦合和 Z 玻色子一样）的质量下限为 4.7 TeV，Z'_{ψ}（来自于 GUT 模型）的质量下限为 4.1 TeV，见图17。具体的研究过程和结果可参见 **??**。

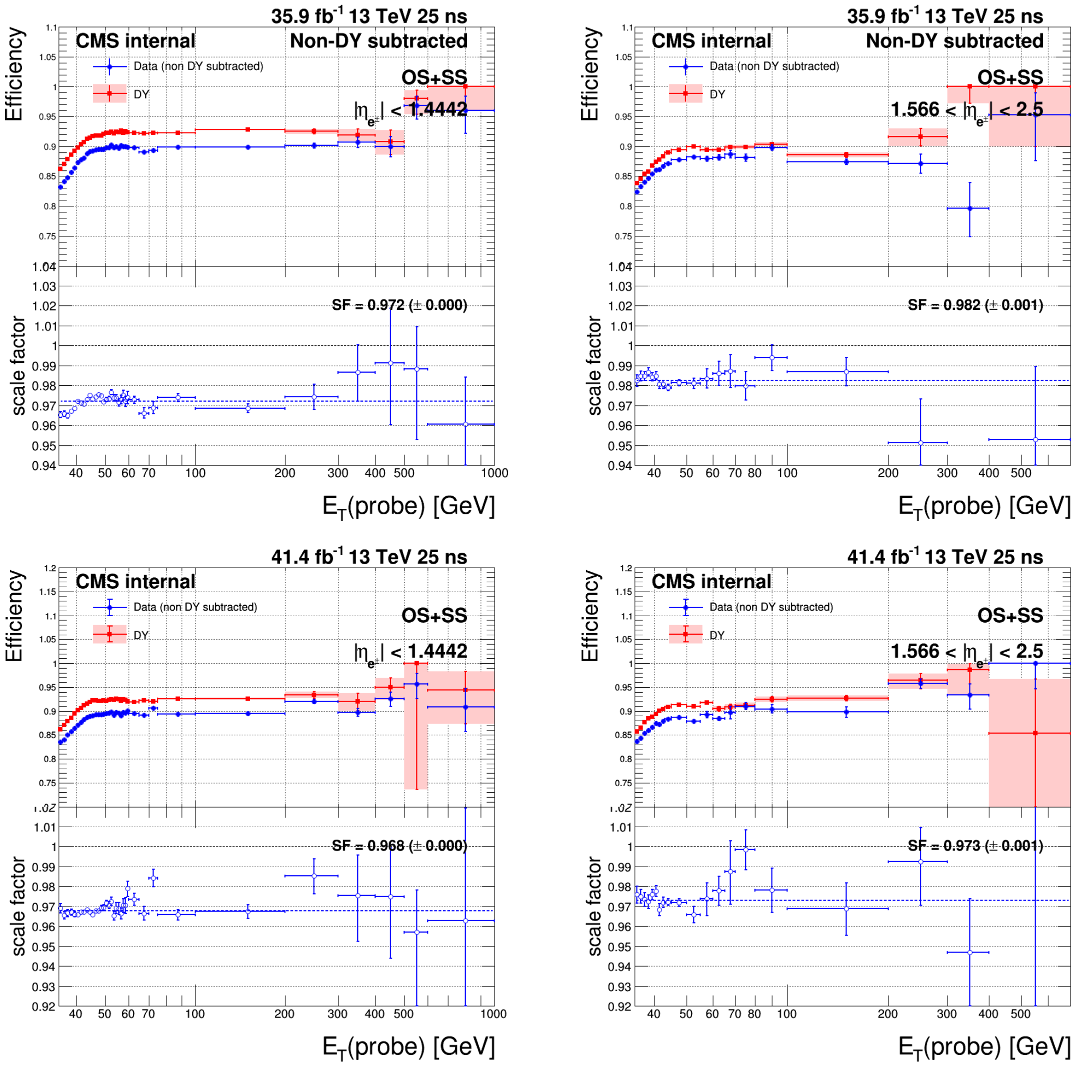

Figure 12: HEEP 条件对桶部（左侧）和端盖（右侧）电子在数据和蒙卡样本（MC）中的选择效率和 scale factor 在 2016（上面）和 2017 年（下面）。

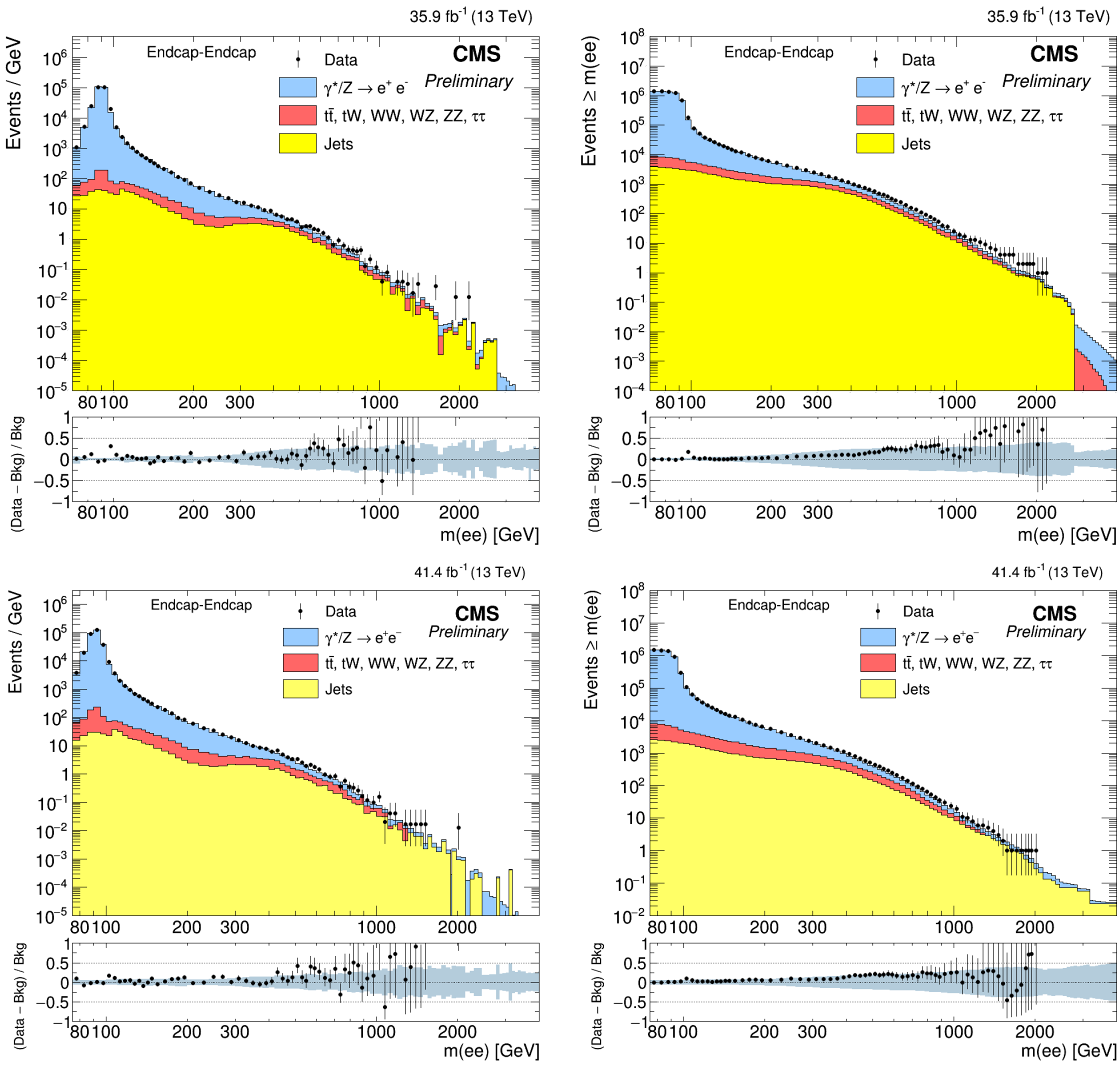

Figure 13: 两电子都在端盖时的双电子不变质量谱（左）和质量谱积分（右）在 2016 年（上）和 2017 年（下）。

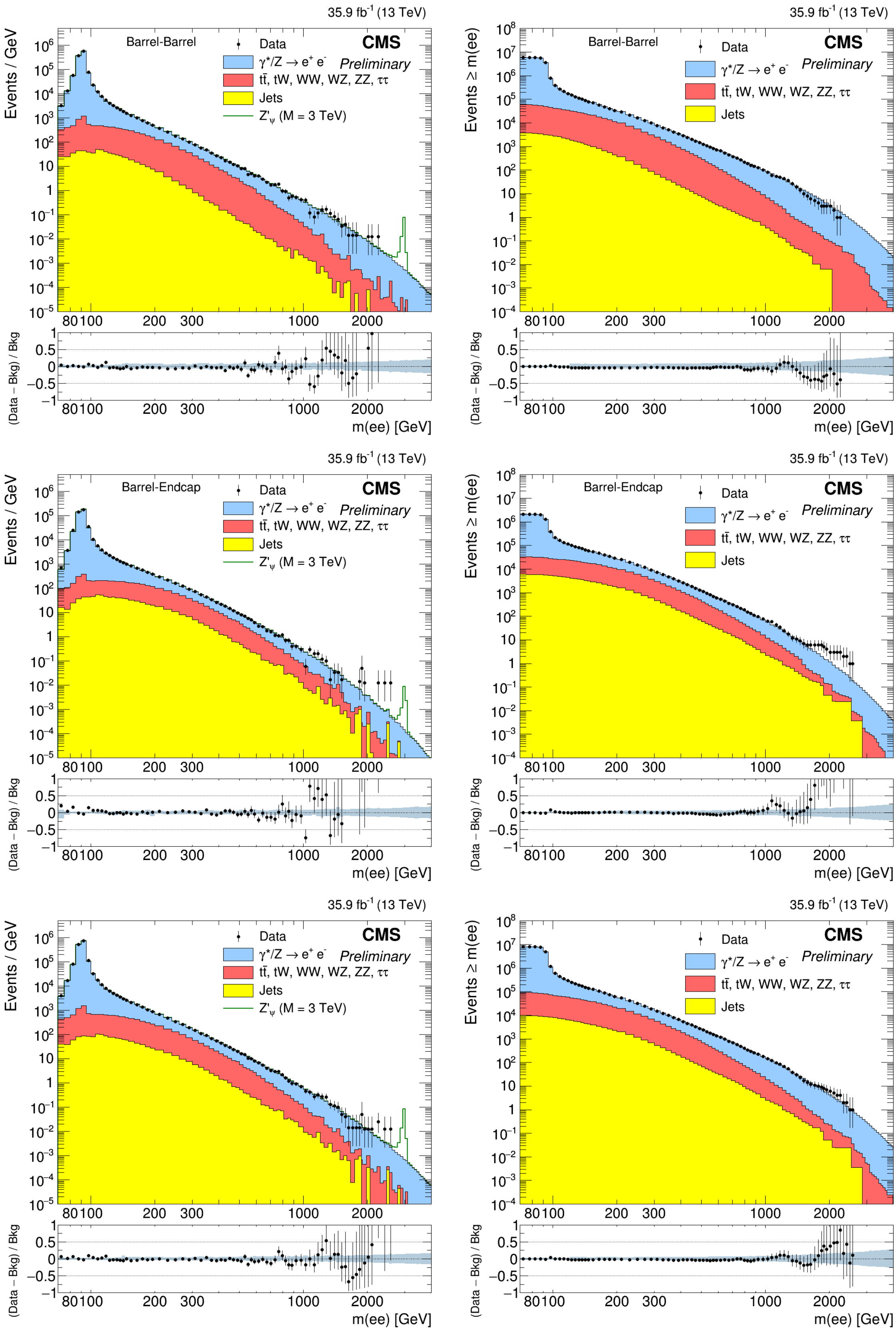

Figure 14: 2016 年的最终双电子不变质量谱（左）和不变质量谱积分（右）对于两电子都在桶部（上）、一个电子在桶部一个电子在端盖（中）和一个电子在桶部（下）的情况。

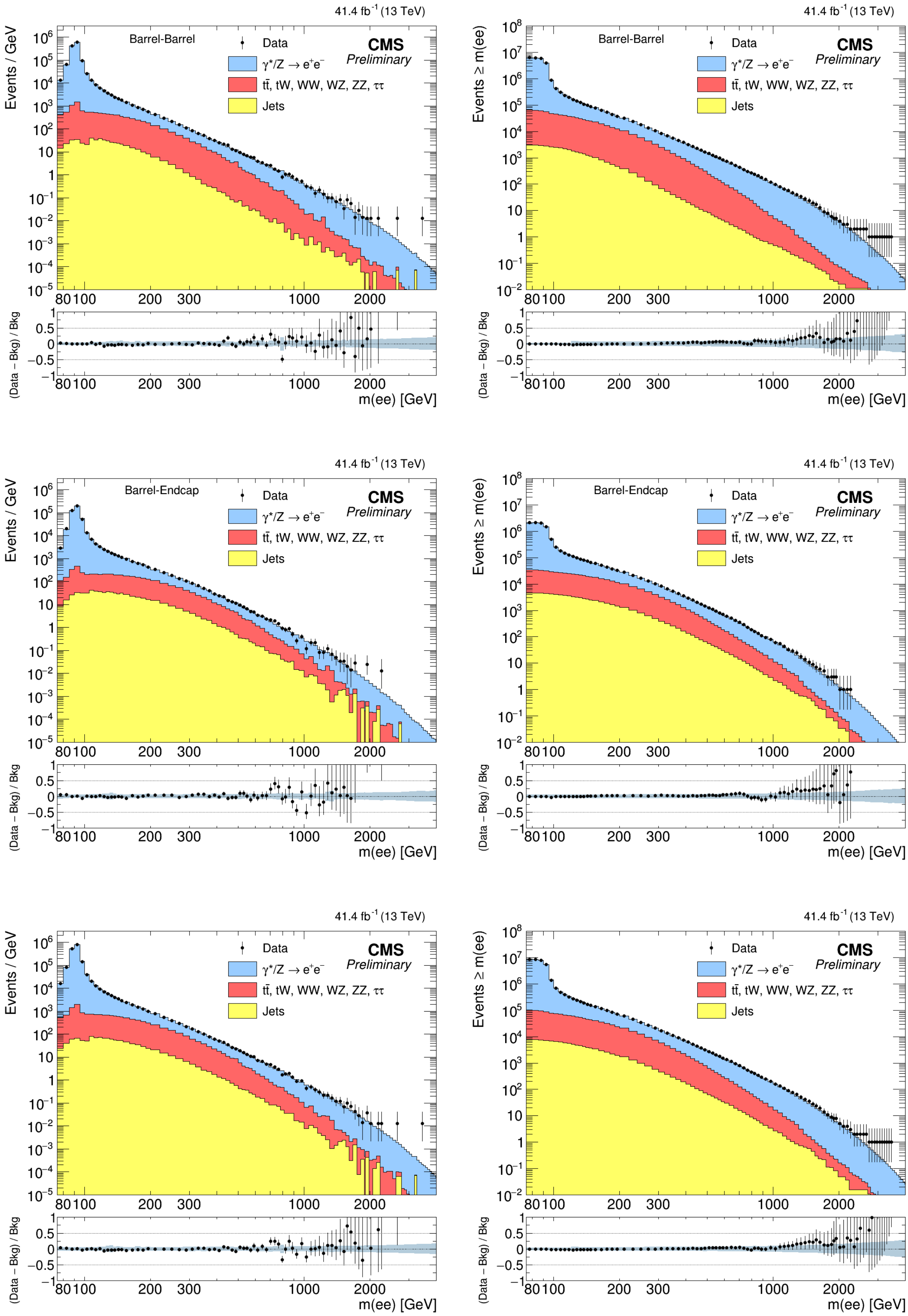

Figure 15: 2017 年的最终双电子不变质量谱（左）和不变质量谱积分（右）对于两电子都在桶部（上）、一个电子在桶部一个电子在端盖（中）和一个电子在桶部（下）的情况。

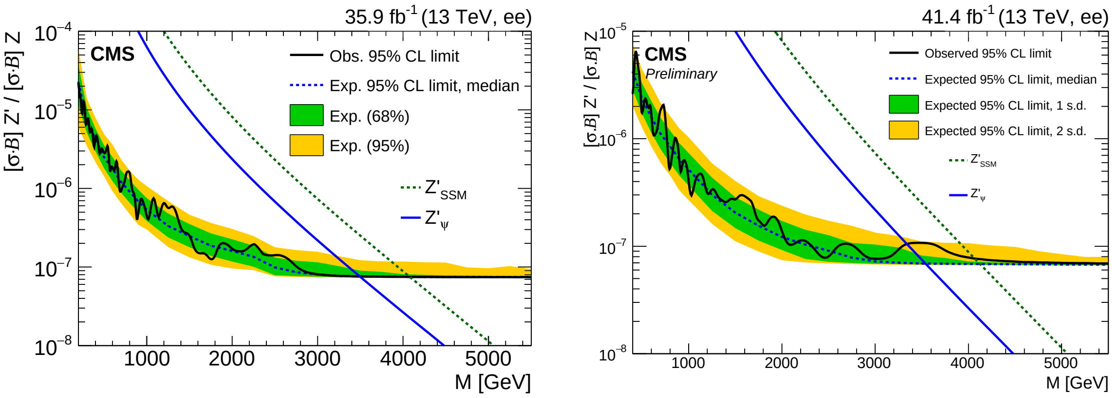

Figure 16: 观测到的和期望的 Z' 的产生截面乘以衰变分支比的 95% 上限在 2016 年（左）[31] 和 2017 年（右）[32]，同时给出了 Z'_{SSM} 和 Z'_{ψ} 对应的理论值。

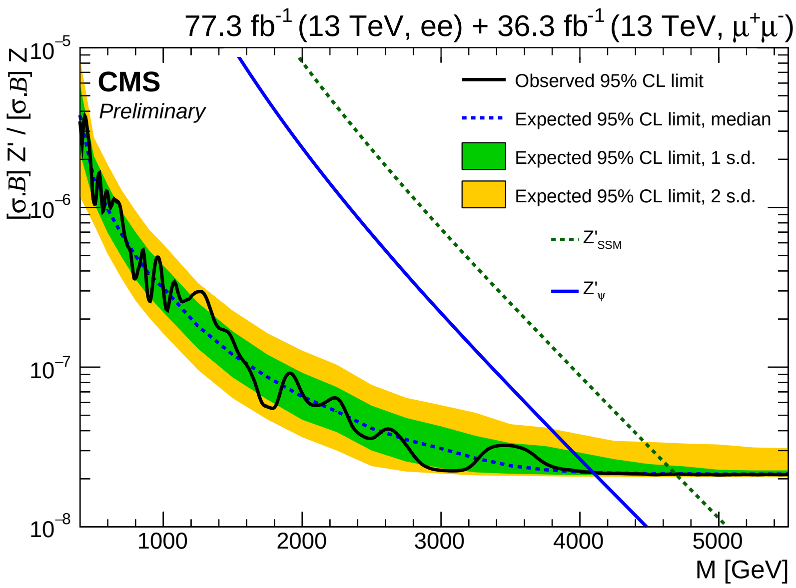

Figure 17: 在结合 2016 年双电子和双谬子道的数据以及 2017 年双电子道的数据后观测到的和期望的 Z' 的产生截面乘以衰变分支比的 95% 上限，同时给出了 Z'_{SSM} 和 Z'_{ψ} 对应的理论值[32]。

在 top 夸克产生过程寻找新物理

在介绍该物理分析之前有必要先介绍一下该物理的总体进展。 LHC 上的 CMS [44, 45] 和 ATLAS [46, 47] 实验组以及 Tevatron 上的 D0 [48] 实验组曾利用单顶夸克 t-channel 产生过程和顶夸克衰变过程寻找 Wtb 的奇异耦合。此外 CMS 曾利用 7 TeV 的数据通过顶夸克对产生过程寻找过新的夸克胶子耦合。最后， LHC [44, 49] 和 Tevatron [50, 51] 也对顶夸克参与的味改变中性流过程的进行了广泛的寻找。

本论文的第二个研究课题是通过双电子或双缪子并且伴随几个 jet（即喷注） 或 bjet（也叫 btag，为含底夸克的喷注） 的末态对顶夸克的产生过程是否存在新物理进行寻找，包括了顶夸克对的产生过程（$\mathrm{t\bar{t}}$ ）和一个顶夸克加上一个 W 玻色子的过程（tW）。利用的数据是来自 CMS 的 2016 年 35.9 fb^{-1} 的数据。被选中的电子或缪子需要通过好电子和好缪子的鉴别，同时电子或缪子的横动量要大于 20 GeV，其中 leading 的电子或缪子的横动量要大于 25 GeV。此外，双电子或双缪子的电荷需要相反，整个事例需要通过相关的触发表。为了去除 Drell-Yan 本底过程，要求双电子或双缪子的不变质量需要在 Z 玻色子质量区间外，同时该事例的 MET 要大于 60 GeV。但在实验中发现数据的 MET 分布和蒙卡样本中 MET 的分布符合的并不好，因此采用了 data-driven 方法去估计数据中的 Drell-Yan 本底事例数。我们利用蒙特卡洛样本来模拟能产生两个真电子或真缪子的过程，例如 $\mathrm{t\bar{t}}$ 、tW 和双玻色子过程，对于存在的 jet 误判为电子或缪子的过程，我们利用 “same-sign” 的 data-driven 方法去估计。经过事例选择后的双电子道和双缪子道中 leading 轻子的 Pt、η 和 ϕ 的分布可见图 18。双电子道和双缪子道中 sub-leading 轻子的 $\mathrm{p_T}$ 、η 和 ϕ 的分布可见图19。从中可见数据的分布与蒙特卡洛样本的预期一致。

最终的双电子道和双缪子道中数据和蒙卡样本在不同 jet 和 bjet 区域的事例数可见图 20。从中我们知道 tW 过程的事例主要出现在 1-jet,1-tag 区域，而 2-jet,1-tag 和 ≥2-jet,2-tag 的区域主要来自 $\mathrm{t\bar{t}}$ 过程。

该分析主要寻找了几种可能存在的新耦合，其中包括只参与 tW 过程的 $\mathrm{C_{tW}}$ （此表示右手的 W 玻色子和 top 夸克及 b 夸克的相互作用），$\mathrm{C_{\phi q}^{(3)}}$ （此与标准模型的 W 玻色子和 top 夸克及 b 夸克相互作用一致），$\mathrm{C_{uG}}$ （此表示胶子与 u 夸克和 top 夸克的相互作用）和 $\mathrm{C_{cG}}$ （此表示胶子与 c 夸克和 top 夸克的相互作用）以及只参与 $\mathrm{t\bar{t}}$ 过程的 $\mathrm{C_G}$ （此表示三个胶子的相互作用）和两个过程都参与的 $\mathrm{C_{tG}}$ （此表示胶子与两 top 夸克的相互作用）。这些过程的费曼图可见图 21。

由于 $\mathrm{t\bar{t}}$ 和 tW 过程末态很相似，因此该分析采用了多变量分析（神经网络）的方法来区分 $\mathrm{t\bar{t}}$ 和 tW 事例，从而提高了该分析对新物理的敏感度。最终的神经网络输出可见图22。

可惜从图 22 中看到实验数据的分布和标准模型预测一致，并没有发现新物理的迹象。在最后该分析利用统计学的方法给出了不同耦合的 95% 的置信区间。在结合了一个类似的分析道即一个电子加一个缪子道后，最终的不同耦合的 95% 的置信区间可见图 23。该分析首次对 $\mathrm{C_G}$ 给出了限制，也提高了之前 $\mathrm{C_{tG}}$ 的结果，关于 $\mathrm{C_{tW}}$ ，$\mathrm{C_{\phi q}^{(3)}}$ ，$\mathrm{C_{uG}}$ 和 $\mathrm{C_{cG}}$ 则是首次利用 tW 过程对其进行研究，也是对之前来自单顶夸克过程的研究结果的补充。关于该分析的更加具体的研究过程和结果可参见 **??**。

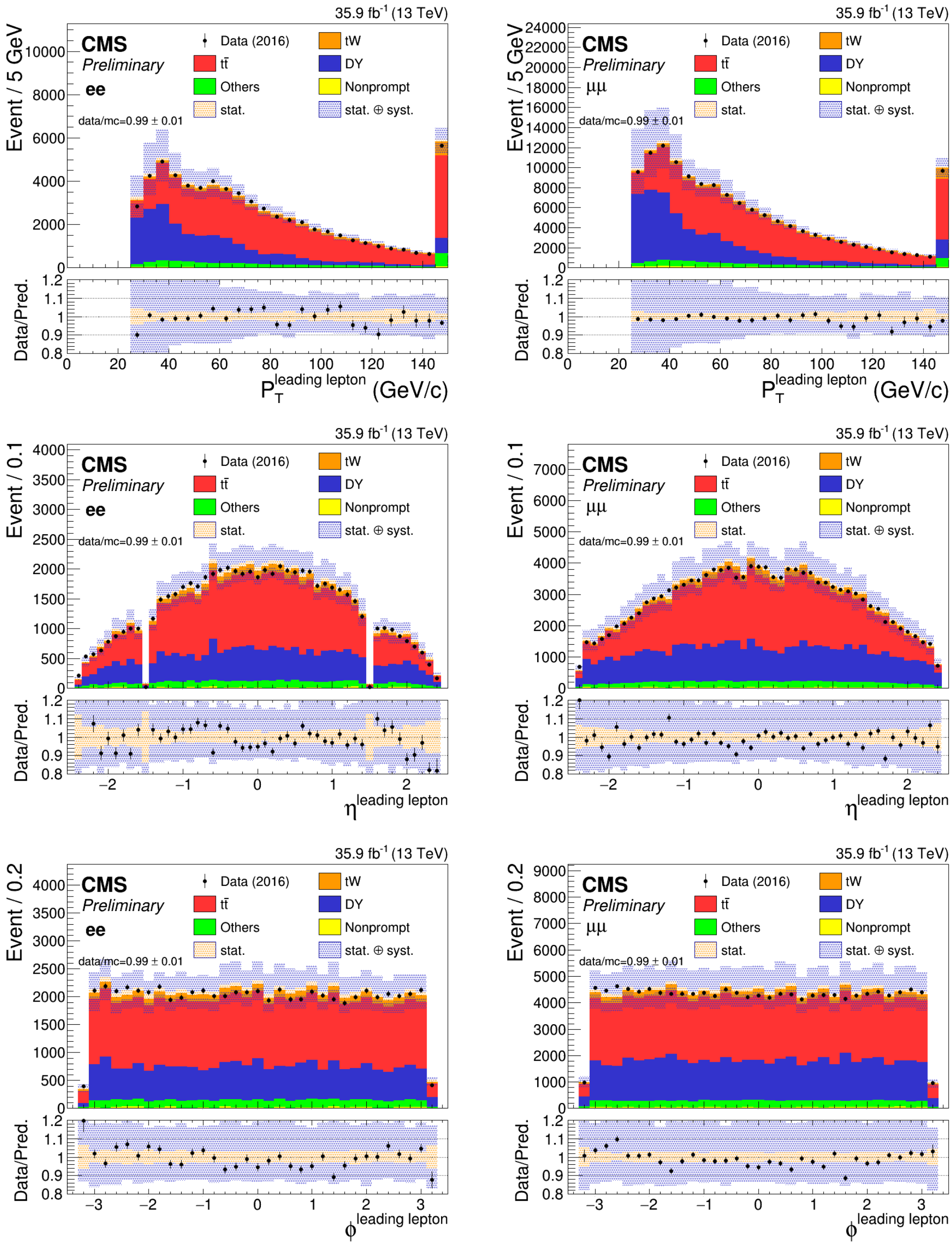

Figure 18: 双电子道（左）和双缪子道（右）中 leading 轻子的 Pt （上）、η （中）和 ϕ （下）的分布。

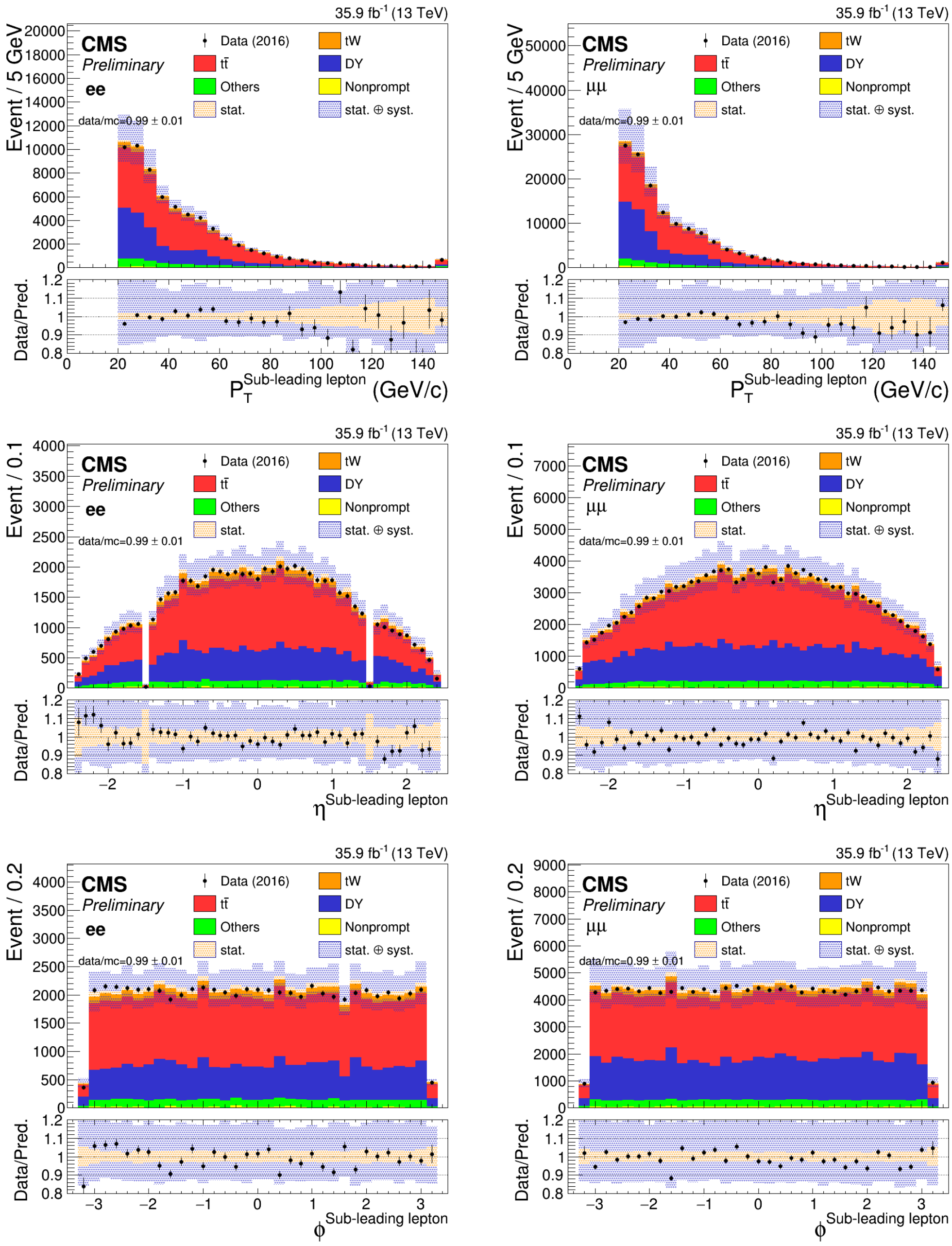

Figure 19: 双电子道（左）和双缪子道（右）中 sub-leading 轻子的 Pt （上）、η （中）和 φ （下）的分布。

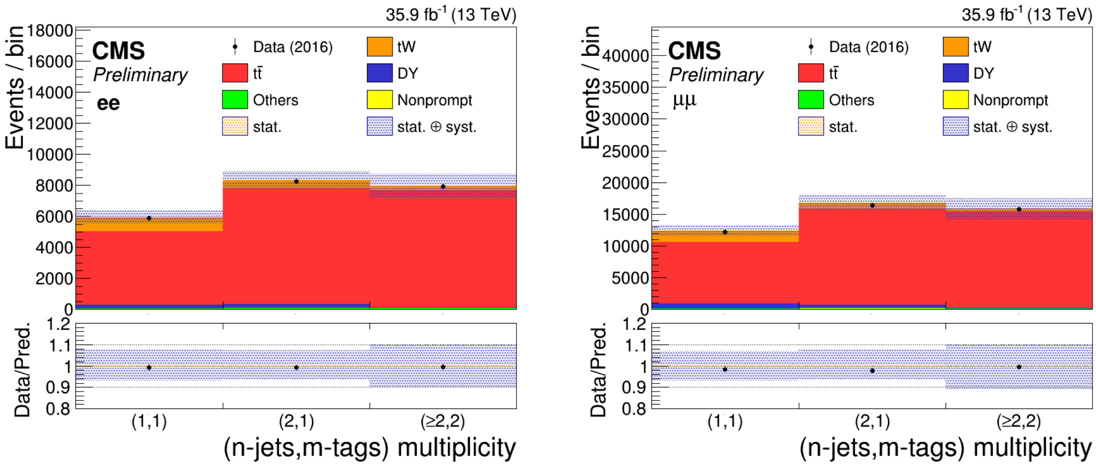

Figure 20: 双电子道（左）和双缪子道（右）中数据和蒙卡样本在不同 jet 和 bjet区间的事例数。

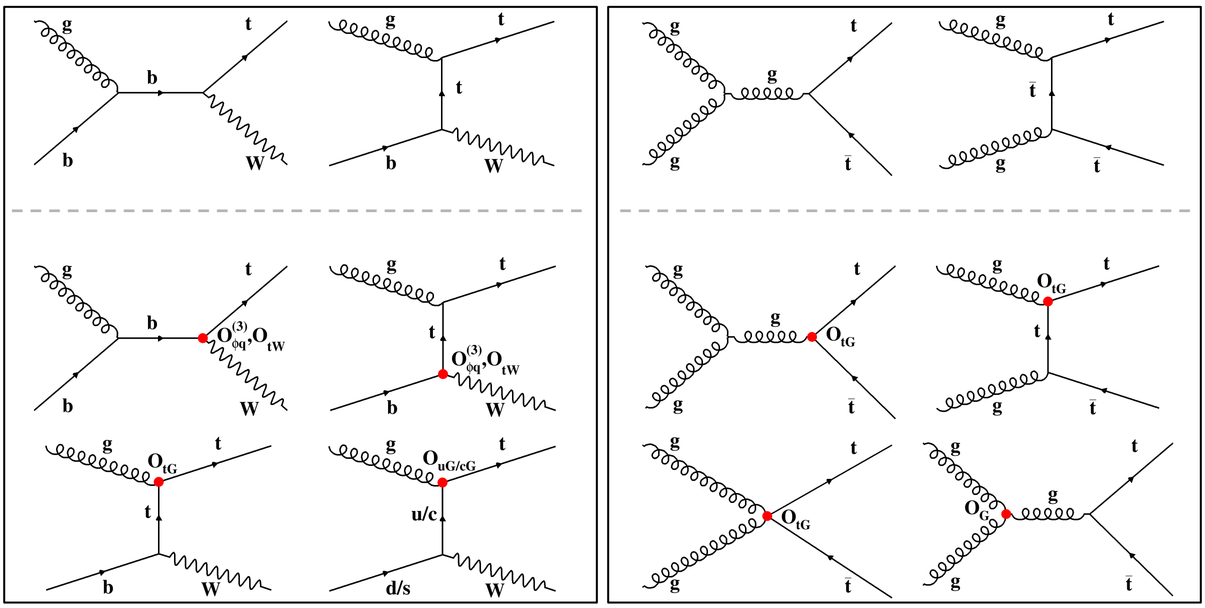

Figure 21: tW（左）和 $t\bar{t}$ （右）的领头阶费曼图。第一行为标准模型过程，第二行和第三行分别代表含有 $O_{\phi q}^{(3)}$ 、O_{tW} 、O_{tG} 、O_{G} 和 $O_{u(c)G}$ 的过程。

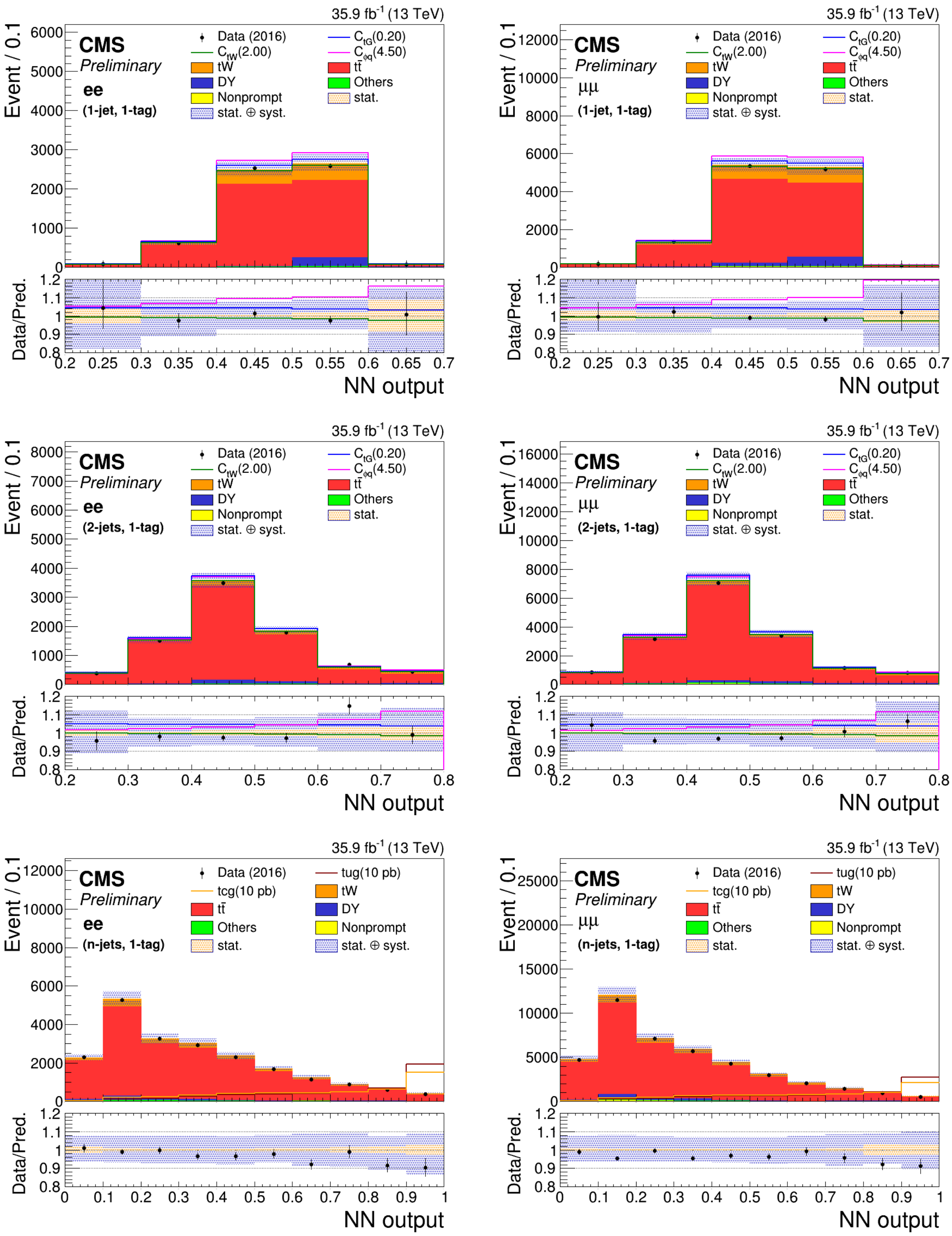

Figure 22: 数据和蒙特卡洛样本在双电子道（左）和双缪子道（右）在 1-jet,1-tag （上）、2-jet,1-tag （中）和 n-jets,1-tag （下）区域的神经网络（Neural Network）输出。

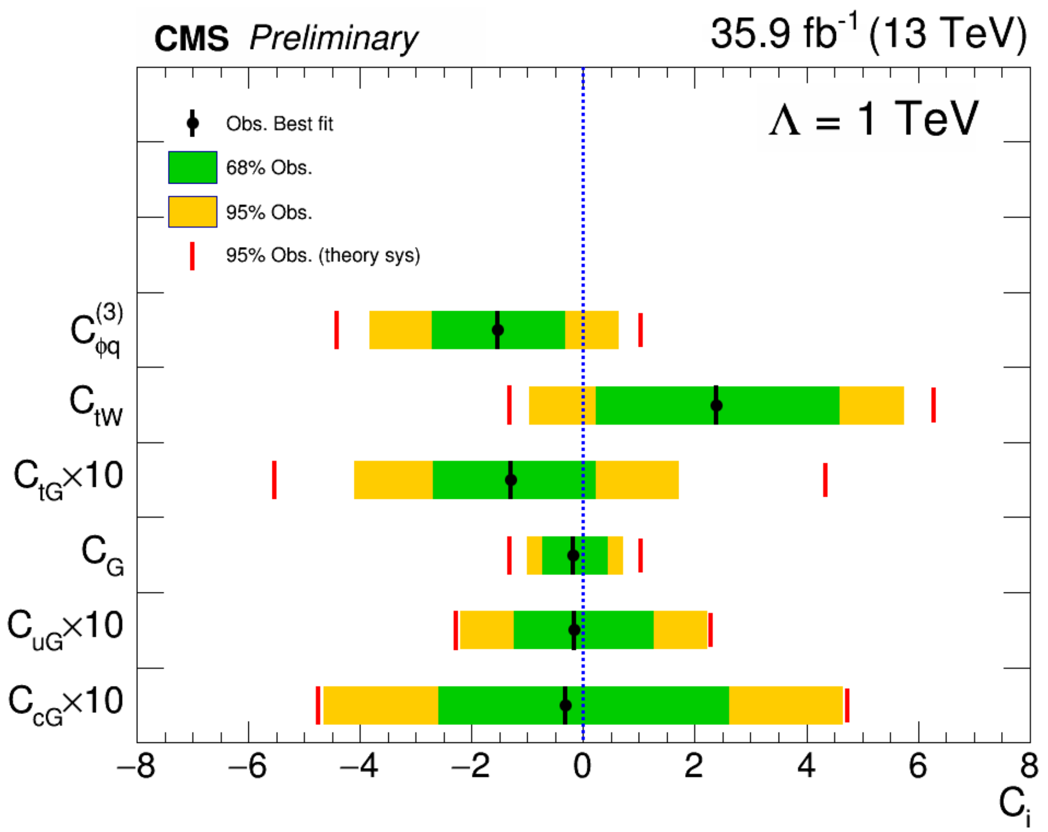

Figure 23: 在结合双电子道、双缪子道和一个电子加一个缪子道后观测到的和预测的不同耦合的 95% 的置信区间 [52]。

Introduction

What is the origin of matter? What are the most fundamental elements in our universe? What are the main forces between matter? These are interesting, basic, and important questions. Although they are difficult to be answered, we are on the way to find the answers.

Particle physics is a subject that tries to find the basic particles in the Universe and to understand the interaction mechanisms between these fundamental particles. The most well known and successful theory in particle physics is the Standard Model (SM) which managed to explain until now all the experimental observations with outstanding precision. The final missing piece of the SM, the "Higgs" particle which was introduced in 1964 by Brout, Englert, and Higgs in order to explain the origin of masses of elementary particles, has been discovered in 2012 (48 years after its prediction) at a mass of around 125 GeV by the ATLAS and CMS experiments at the Large Hadron Collider (LHC).

The LHC is the largest hadron collider in the world providing proton-proton collisions with the highest center-of-mass energy ever achieved (13 TeV from 2015 to 2018). There are four main experiments at the LHC, two of them CMS and ATLAS are general purpose detectors. The discovery of the Higgs boson by joint efforts of the ATLAS and CMS collaborations is one of the most important achievements of modern particle physics research and accomplished one of the main goals of the LHC program.

Nevertheless, besides the tremendous successes of the SM, it is not able to describe the full picture of Nature. Indeed, it does not show candidates of dark matter and dark energy, it does not predict the oscillation of neutrinos, it does not have a good explanation for the asymmetry between matter and antimatter. It has in addition some issues of internal consistency, such as the hierarchy problem, a large number of free parameters and so on. Therefore, the SM is generally considered as an effective theory of a more fundamental theory at high energy. In order to address some shortcomings of the SM, several models that go beyond the SM have been proposed, such as supersymmetric models (SUSY), which provide a candidate of dark matter and provide an explanation to the Higgs mass fine-tuning problem, or The Grand Unified Theory (GUT) which tries to unify electromagnetic, weak, and strong interactions into one interaction through extensions of the SM gauge group, or the large extra dimensions theory, which involves additional spatial dimensions to explain the weakness of the gravitational force compared to the other forces. These beyond SM models typically introduce new neutral bosons heavier than the standard model Z boson, which are generically called Z' bosons.

If the mass scale of such new particles are reachable in collider experiment, these particles would manifest themselves as a localised excess of events in the observed invariant mass spectra. In this thesis, direct search for new heavy resonances decaying into the dielectron final state has been performed using the CMS detector. This channel has the advantage that electrons can be reconstructed and identified with high efficiency which leads to a low background contamination coming from misreconstructed electron candidates. Besides, the main component of SM background in this channel is Drell-Yan process, which is well understood and its rate is small in the high mass region. These facts give a strong motivation for searching for new heavy resonances in the dielectron final state. In this thesis, the analysis of data collected by the CMS experiment during years 2016 and 2017 are reported.

However, if the new physics scale is not reachable at the LHC, new physics could affect SM interactions indirectly, through modifications of SM couplings or enhancements of rare SM processes. Due to its large mass, close to the electroweak symmetry breaking scale, the top quark is expected to play an important role in several new physics scenarios. An effective field theory (EFT) approach which is a model-independent approach is used in this thesis to search for new physics in the top quark sector in the dilepton (ee, $\mu\mu$) final states using the data collected by CMS in 2016.

The thesis is organised as follows. The SM of particle physics is introduced in Chapter 1, including a description of fundamental particles, the forces between these particles, the main properties of the SM Drell-Yan process and an introduction to the EFT theory. Chapter 2 lists the shortcomings of the SM and addresses how various theories beyond the SM propose to solve them. In particular, the models that predict additional massive resonances are introduced. The motivations for searching for new physics in the top quark sector is also given. Chapter **??** presents an introduction to the LHC machine, including its design and operational parameters, as well as the phenomenological aspects of the proton-proton interactions. The CMS detector is also introduced in detail in this chapter. The reconstruction of the different particles produced in the proton proton collisions in CMS is explained in Chapter **??**. Chapter **??** describes in detail the results of the search for new resonances decaying into the dielectron final state and all the aspects of the analysis are covered. The results of the search for new physics in the top quark sector are shown in Chapter **??**, covering as well all the aspects of the analysis. Finally, Chapter **??** exposes the conclusions coming from both searches.

Chapter 1

The Standard Model of particle physics

This chapter introduces the Standard Model of particle physics which describes the family of elementary particles and the three of the four fundamental forces of Nature with corresponding mediators. After that, the gauge symmetry is briefly expressed. Then, the Drell-Yan process is introduced in details due to its importance in this thesis. In Addition, the photon induced process is also shortly discussed. Finally, the effective field theory which will be used in this thesis is presented.

1.1 The elementary particles

It has been long time for people to understand what are the basic objects which constitute our world. From Demokritos (470-380 BC) who thought matter was built of discrete building blocks to John Dalton (1766-1844) who came up with the matter made of atoms. In the early 1900's J.J. Thomson proposed a so called "plum pudding model" which assumes the atom was a uniform sphere of positively charged matter in which electrons were embedded. However in 1910 Ernest Rutherford and his colleagues performed α ray scattering experiments and found that the whole mass and all positive charges of the atom were concentrated in a minute space at the centre which is called "nucleus". After the discovery of the neutron in 1932 by James Chadwick, models for a nucleus composed of protons and neutrons were quickly developed by Dmitri Ivanenko and Werner Heisenberg. Furthermore in 1968 the deep inelastic scattering experiments at the Stanford Linear Accelerator Center provided the first convincing evidence of the reality of quarks in the proton or neutron. In the Standard Model (SM) [1, 2, 3] the quarks are the elementary particles and there are six different kinds of flavors for the quarks called up (u), down (d), charm (c), strange (s), top (t), and bottom (b). The mass, charge, and spin of the quarks are shown in Table 1.1, here the e means one electron's charge which equals 1.6×10^{-19} C. The quarks are categorized in there generations according to their masses and charges. Besides it is verified that the quarks have another property which is called the "color charge", a quark can be "Red" or "Blue" or "Green". Moreover all the quarks have its anti-quark partner which has opposite quantum numbers with regard to the quark including flavor, charge, and color charge. Therefore there are $6\ (\text{flavor}) \times 3\ (\text{color}) \times 2\ (\text{anti} - \text{quark}) = 36$ kinds of quarks in the SM and all the hadrons are composed by quarks or anti-quarks. For meson it is composed by $q\bar{q}$ and for baryon it is composed by qqq or $\bar{q}\bar{q}\bar{q}$.

Similar to the quark family, there is a lepton family and the most common lepton is the electron which exists as a cloud out of nucleus to form an atom. All the leptons are shown in Table 1.2 with their charges, spins, and masses. They are electron (e), electron neutrino (ν_e), muon (μ), muon neutrino (ν_μ), tau (τ), and tau neutrino (ν_τ). The leptons

Generation	Quark	Charge	Spin	Mass
First	up quark (u)	2/3 e	1/2	$2.3^{+0.7}_{-0.5}$ MeV
	down quark (d)	-1/3 e	1/2	$4.8^{+0.5}_{-0.3}$ MeV
Second	charm quark (c)	2/3 e	1/2	1.275 ± 0.025 GeV
	strange quark (s)	-1/3 e	1/2	95 ± 5 MeV
Third	top quark (t)	2/3 e	1/2	$173.21 \pm 0.51 \pm 0.71$ GeV
	bottom quark (b)	-1/3 e	1/2	4.66 ± 0.03 GeV

Table 1.1: Quarks and their properties [53].

Generation	Lepton	Charge	Spin	Mass
First	electron (e)	-e	1/2	511 MeV
	electron neutrino (ν_e)	0	1/2	< 2 eV
Second	muon (μ)	-e	1/2	105.67 MeV
	muon neutrino (ν_μ)	0	1/2	< 2 eV
Third	tau (τ)	-e	1/2	1776.99 MeV
	tau neutrino (ν_τ)	0	1/2	< 2 eV

Table 1.2: Properties of the leptons in the three generations. Neutrinos are assumed to have zero mass in SM but by the observation of neutrino's oscillations the upper limits on their masses are set [53].

are also categorized into three generations and each generation has its own lepton flavor. The first generation has electron flavor, the second generation has muon flavor, and the third generation has tau flavor. For neutrinos they are always left handed and they are very hard to be detected because of the very weak interaction between the matter and neutrinos. In SM the neutrinos are assumed to be massless while in experiment we have observed the neutrino oscillations which means the neutrinos have masses, so the study of neutrinos may bring us the new theory beyond the SM. Similar with the quarks, all the leptons also have theirs anti-particle partners which own the opposite quantum numbers. While unlike the quarks, the leptons do not have color charge property. Therefore there are $6 \times 2 = 12$ kinds of leptons in SM.

Now that all the spin 1/2 (fermion) elementary particles in SM have been introduced, the interactions between these particles and the mediators will be discussed in the next section.

1.2 The fundamental interactions

It is well known that there are four characteristic interactions among fundamental particles.

1. Electromagnetic interaction : It is mediated by massless photon ($m_\gamma = 0$) with spin $= 1$ among charged particles. Because of the massless of photon the interacting range of electromagnetic interaction is infinite. The theory to describe the electromagnetic interaction is quantum electrodynamics (QED) which has been well understood. QED is renormalizable, for example the divergence from vacuum polarization and higher order loop contributions can be absorbed into the physical charge of particle. The coupling constant is $\alpha = \frac{e^2}{4\pi\varepsilon_0\hbar c} \simeq \frac{1}{137}$ which characterizes the strength of the coupling of charged particle with the electromagnetic field. Because of the smallness of α, the perturbation development works well for QED.
2. Strong interaction : It is mediated by massless gluons ($m_g = 0$) with spin $= 1$. This interaction can only happen between quarks and gluons. The theory that describes

the strong interaction is called quantum chromodynamics (QCD). For strong interaction the coupling strength is also running but in an opposite way as the electromagnetic interaction, which means that the coupling will decrease when the interaction energy increases. Because of that there is one special phenomenon for strong interaction called "asymptotic freedom" which means quarks and gluons behave like free particles when the interaction energy is very high. At high energy the perturbation theory works well because of "asymptotic freedom" but it is not the case at low energy (below the GeV). Therefore there are still a lot of works needed to be done for understanding QCD process at low energy. Another special phenomenon of the strong interaction is called the "color confinement", which means there are no free quarks in the world. The quarks need to be grouped to form a colorless hadron. For instance the baryon is formed by red, green, and blue quarks and the meson is formed by red and anti-red quarks or blue and anti-blue quarks or green and anti-green quarks.

3. Weak interaction : It is mediated by massive weak bosons ($m_{W^{\pm}} \cong 80.4$ GeV, $m_Z \cong 91.2$ GeV) with spin = 1. Because of the heavy mediator, its interacting range is very short, which is $\sim 10^{-18}$ m. The coupling strength of weak interaction is the weakest among electromagnetic and strong interactions. Although the coupling strength is small, some processes can only happen via weak interaction like flavor changing or neutrino involved processes.

4. Gravitational interaction : It is mediated by massless gravitons ($m_G = 0$) with spin = 2 among all massive particles. Because of its very small coupling strength we normally do not consider gravitational interaction in high energy physics. In macroscopic world the gravitation is important, such as it makes an apple falling.

The summary of interaction range, relative strength, and mediator for the four fundamental interactions is shown in Table 1.3. Last but not least, in the SM the origin of mass of the elementary particles is coming from interactions between particles and the Brout-Englert-Higgs scalar field (the so called "Higgs" boson). In 2012 the ATLAS [4] and CMS [5] experiments observed such a particle and the mass is ~ 125 GeV.

The summary of all elementary particles, force carries, and Higgs boson is shown in Figure 1.1.

Interaction	Range	Relative strength	Mediators
Strong	10^{-15} m	1	8 gluons (g)
Electromagnetic	∞	10^{-3}	photon (γ)
Weak	10^{-18} m	10^{-14}	W^+, W^-, Z
Gravitational	∞	10^{-43}	graviton (G) ?

Table 1.3: Range, relative strength with respect to the strong force, and mediators of the four fundamental interactions. The gravitational force is not included in the SM, and gravitons are hypothetical particles.

An introduction about the Feynman calculus is presented in Appendix ??. Besides, more detailed introductions about the QED and the QCD are presented in Appendix ?? and Appendix ??, respectively. The group theory is briefly introduced in Appendix ??.

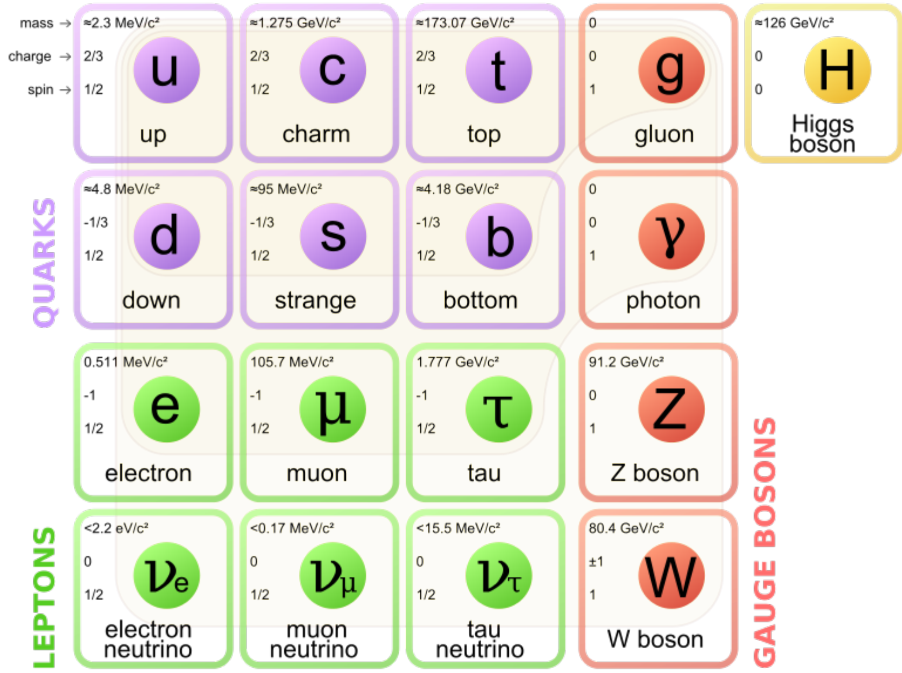

Figure 1.1: Overview of the Standard Model constituents: the quarks and leptons, the gauge bosons and the Higgs boson.

1.3 Gauge symmetries: a brief introduction

The formulas in this section are from book [54].

The Lagrangian

As we know, in classic physics, the motion equation of a particle can be obtained from the Lagrange's equation

$$\frac{d}{dt}(\frac{\partial L}{\partial \dot{q}_i}) - \frac{\partial L}{\partial q_i} = 0 \tag{1.1}$$

where the q_i are the generalized coordinates of the particle, t is the time variable and $\dot{q}_i = dq_i/dt$. The $L \equiv T - V$, where T is kinetic energy of the particle and V is the potential energy of the particle. The Lagrange's equation 1.1 can be extended from describing the motion of one particle to describe the motion of a field $\phi(t, \mathbf{x})$ (which has a value at every point in space that changes in time) by replace q_i and $\dot{q}_i$ with ϕ and $\partial\phi/\partial x_\mu$ respectively, here the $x_\mu \equiv (t, \mathbf{x})$. Therefore, we obtained the Lagrange's equation for field ϕ as

$$\frac{\partial}{\partial x_\mu}(\frac{\partial \mathcal{L}}{\partial(\partial\phi/\partial x_\mu)}) - \frac{\partial \mathcal{L}}{\partial \phi} = \frac{\partial}{\partial t}(\frac{\partial \mathcal{L}}{\partial(\partial\phi/\partial t)}) + \sum_{i=1}^{3} \frac{\partial}{\partial x_i}(\frac{\partial \mathcal{L}}{\partial(\partial\phi/\partial x_i)}) - \frac{\partial \mathcal{L}}{\partial \phi} = 0, \tag{1.2}$$

which is called Euler-Lagrange equation and the $\mathcal{L}$ is Lagrangian density with

$$L = \int \mathcal{L} d^3x.$$

Usually we call $\mathcal{L}$ itself the Lagrangian.

For example, the Dirac Lagrangian (which describes the spin $\frac{1}{2}$ particle in quantum mechanics) is

$$\mathcal{L} = i\overline{\psi}\gamma_\mu\partial^\mu\psi - m\overline{\psi}\psi \tag{1.3}$$

where ψ is the particle field and $\overline{\psi} \equiv \psi^\dagger\gamma^0$, m is the mass of the particle, the $\partial^\mu = (\frac{\partial}{\partial t}, -\nabla) = (\frac{\partial}{\partial t}, -\frac{\partial}{\partial x_1}, -\frac{\partial}{\partial x_2}, -\frac{\partial}{\partial x_3})$, $\gamma_\mu = (\gamma_0, \gamma_1, \gamma_2, \gamma_3)$ are the gamma matrices:

$$\begin{gathered}
\gamma_0 = \begin{pmatrix} 1 & 0 \\ 0 & -1 \end{pmatrix}, \ \gamma_i = \begin{pmatrix} 0 & -\sigma_i \\ \sigma_i & 0 \end{pmatrix} \quad \text{with } i \ = \ 1, \ 2, \ 3 \\
\sigma_1 = \begin{pmatrix} 0 & 1 \\ 1 & 0 \end{pmatrix}, \ \sigma_2 = \begin{pmatrix} 0 & -i \\ i & 0 \end{pmatrix}, \ \sigma_3 = \begin{pmatrix} 1 & 0 \\ 0 & -1 \end{pmatrix}
\end{gathered} \tag{1.4}$$

Symmetry and conservation

The first person who linked symmetry with conservation law is Emmy Noether [55]. She pointed out that each symmetry (which means the physics or the Lagrangian is invariant under this operation) corresponds to one conserved quantity. For example, the symmetries of transitions, time displacements, and rotations lead to the conservation of momentum, energy and angular momentum. An example about "internal" symmetry is given below.

Suppose we change the phase of electron field by

$$\psi \to e^{i\alpha}\psi, \tag{1.5}$$

where α is space and time independent. It is easily to see that this operation is a symmetry operation (usually called global $U(1)$ symmetry, because all these kind of operations with different α value form a unitary group with one group generator, the global means α is space and time independent) due to the invariance of Lagrangian (see Equation 1.3). From Noether's theorem we know there is a conserved quantity corresponding to this symmetry.

According to the property of $U(1)$ group, when α is infinitesimal the Equation 1.5 can be written as

$$\psi \to (1 + i\alpha)\psi. \tag{1.6}$$

and by asking the invariance of Lagrangian we get

$$0 = \delta\mathcal{L} = \frac{\partial}{\partial\psi}\delta\psi + \frac{\partial}{\partial(\partial_\mu\psi)}\delta(\partial_\mu\psi) + \frac{\partial}{\partial\overline{\psi}}\delta\overline{\psi} + \frac{\partial}{\partial(\partial_\mu\overline{\psi})}\delta(\partial_\mu\overline{\psi}) \tag{1.7}$$

and finally we can get can a conserved current from

$$\partial_\mu j^\mu = 0, \tag{1.8}$$

where

$$j^\mu = \frac{ie}{2}(\frac{\partial}{\partial(\partial_\mu\psi)}\psi - \overline{\psi}\frac{\partial}{\partial(\partial_\mu\overline{\psi})}) = -e\overline{\psi}\gamma^\mu\psi. \tag{1.9}$$

It can be proved that the conserved current j^μ leads to the charge conservation of the particle.

$U(1)$ local gauge symmetry

As we know, in previous section, the Lagrangian (Equation 1.3) is invariant under $U(\alpha)$ operation, while it will not be the case for local operator $U(\alpha(t,\mathbf{x}))$ which is time and space dependent. However, the real Lagrangian should be invariant with $U(\alpha(t,\mathbf{x}))$, as we know the observation $|\langle\psi|\psi\rangle|^2 = |\langle\psi|U^\dagger U|\psi\rangle|^2$ do not dependent with the phase.

In order to maintain the Lagrangian is invariant under $U(\alpha(t,\mathbf{x}))$, it is needed to replace derivative ∂_μ by D_μ with

$$D_\mu \equiv \partial_\mu - ieA_\mu \tag{1.10}$$

where A_μ transforms as

$$A_\mu \to A_\mu + \frac{1}{e}\partial_\mu\alpha. \tag{1.11}$$

Therefore, the updated Lagrangian will be

$$\mathcal{L} = i\overline{\psi}\gamma^\mu D_\mu\psi - m\overline{\psi}\psi = \overline{\psi}(i\gamma^\mu\partial_\mu - m)\psi + e\overline{\psi}\gamma^\mu\psi A_\mu, \tag{1.12}$$

which means there is an interaction between the field ψ and field A_μ. Actually, it can be proved that the A_μ can be regarded as the photon and after include the kinetic term of the photon (not for the mass term which will break the symmetry) the final Lagrangian for QED is

$$\mathcal{L}_{QED} = \overline{\psi}(i\gamma^\mu\partial_\mu - m)\psi + e\overline{\psi}\gamma^\mu\psi A_\mu - \frac{1}{4}F_{\mu\nu}F^{\mu\nu} \tag{1.13}$$

with

$$F_{\mu\nu} = \partial_\mu A_\nu - \partial_\nu A_\mu \tag{1.14}$$

We have seen that after asking the local $U(1)$ symmetry, a massless gauge boson, the photon, is created.

$SU(3)$ local gauge symmetry

As we know, the quark has three colors (R, G, B) and the Lagrangian

$$\mathcal{L} = \overline{q_i}(i\gamma^\mu\partial_\mu - m)q_i, \quad \text{with } i \ = \ 1,\ 2,\ 3, \tag{1.15}$$

where the q_1, q_2, q_3 denote the three color fields, should be invariant under the color phase transformation (R $\rightleftarrows$ G $\rightleftarrows$ B). This is because we really can't distinguish the exact color of one quark. This color phase transformation can be represented by 3 × 3 traceless unitary matrices U, and all these matrices form a $SU(3)$ ("S" means special because of the zero trace of the matrices) group with 8 generators. The transformation of the quark field under the color phase change can be written as

$$q(t, \mathbf{x}) \to Uq(t, \mathbf{x}) \equiv e^{i\alpha_a(t,\mathbf{x})T_a}q(t, \mathbf{x}), \tag{1.16}$$

where a summation over suffix a from 1 to 8 is implied, the T_a are a set of linearly independent traceless 3 × 3 matrices, and the α_a are the group parameters. Because not all generators T_a commute with each other (e.g. $T_aT_b \neq T_bT_a$), this group is non-Abelian. The conventional choice of T_a matrices are the $\lambda_a/2$ (know as Gell-Mann λ matrices, see Equation **??**). It can be proved that the commutator of any two T_a follows

$$[T_a, T_b] = if_{abc}T_c, \tag{1.17}$$

where f_{abc} are real constant, called the structure constants of the group.

In order to impose the $SU(3)$ color local invariance of the Lagrangian 1.15, we can use the same method described in Section 1.3 by making

$$D_\mu = \partial_\mu + igT_aG^a_\mu, \tag{1.18}$$

and

$$G^a_\mu \to G^a_\mu - \frac{1}{g}\partial_\mu\alpha_a - f_{abc}\alpha_bG^c_\mu. \tag{1.19}$$

Similar with $U(1)$ gauge symmetry, after requiring $SU(3)$ color local symmetry, we created a new gauge field G^a_μ (a=1,...,8) which can be regarded as 8 gluons. After adding the kinetic energy terms of the gluons, the final gauge invariant Lagrangian for QCD process is

$$\mathcal{L}_{QCD} = \overline{q}(i\gamma^\mu\partial_\mu - m)q - g(\overline{q}\gamma^\mu T_aq)G^a_\mu - \frac{1}{4}G^a_{\mu\nu}G^{\mu\nu}_a, \tag{1.20}$$

with

$$G^a_{\mu\nu} = \partial_\mu G^a_\nu - \partial_\nu G^a_\mu - gf_{abc}G^b_\mu G^c_\nu.$$

It should be noticed that due to the non-Abelian of $SU(3)$, the kinetic energy terms $G^a_{\mu\nu}G^{\mu\nu}_a$ induce self-interactions between gauge bosons which is not the case for $U(1)$ gauge symmetry which is Abelian.

We have seen that the exact color $SU(3)$ (or simply $SU(3)_c$) local symmetry gives 8 massless gauge bosons which are gluons, and these gluons can have interactions with the quarks or have self-interactions by QCD process.

$SU(2)_L$ local gauge symmetry and Higgs mechanism

In the weak interaction, the left-handed fermions is coupled to form weak-isospin doublets (e.g. $(\nu_{\mathrm{eL}}, \mathrm{e_L}), (\mathrm{u_L}, \mathrm{d_L})$) and the right-handed fermions form weak-isospin singlet (e.g. $\mathrm{e_R}, \mathrm{u_R}, \mathrm{d_R}$, and there is no right-handed neutrinos). The "rotation" from one fermion to another fermion within the same doublets can be represented by $SU(2)_L$ ("L" means left-handed) group with 3 generators.

As we know, the mediators $W^{\pm}$ boson for weak interaction are heavy particles. If we impose $SU(2)_L$ local symmetry in the same way as we did for $SU(3)$ then we will obtain massless gauge bosons which conflicts with the experimental results. Therefore, we need additional mechanisms to make the gauge bosons have masses. Luckily, in SM we have a mechanism (called "Higgs mechanism") proposed by Brout, Englert and Higgs [56, 57, 58] which suppose there exist a scalar boson (called "Higgs" boson) and its the potential V is not at minimum when its field ϕ at 0, while at value v (called "vacuum expectation value" or simply VEV) the potential reaches minimum, see Figure 1.2 for example.

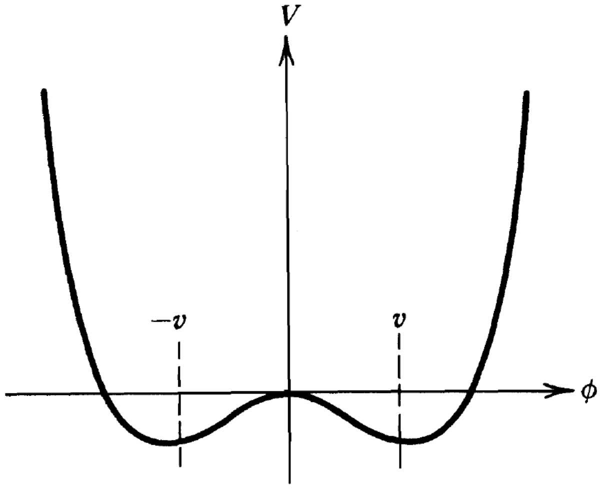

Figure 1.2: An example of one dimension "Higgs" potential [54].

In perturbative calculation we should involve expansions around the minimum energy and this can be done by expanding the ϕ around the v

$$\phi(t, \mathbf{x}) = v + h(t, \mathbf{x}).$$

It means ϕ can be expressed by h, while potential V will not be symmetry under the change of h to $-h$. This makes the "spontaneous symmetry breaking" of ϕ. After expanding the ϕ around the VEV, in new Lagrangian we have a term related to the mass of h (actually is the mass of "Higgs" boson) and a term related to the masses of gauge bosons which means the gauge bosons obtained the masses. By the way, the masses of fermions in SM are also "generated" by Higgs mechanism.

Last but not least, the only $SU(2)_L$ local symmetry does not create the physical Z boson. It is created together with $W^{\pm}$ and photon in $SU(2)_L \times U(1)_Y$ ("Y" means hypercharge, $Y = 2Q - T^3$ with Q is the charge of particle, T^3 is third component of weak-isospin) symmetry which is proposed by Weinberg, Salam, and Glashow [59, 60, 61]. This $SU(2)_L \times U(1)_Y$ gauge invariance theory unifies electromagnetic and weak interactions and is called electroweak theory. Finally, the complete SM theory is based on $SU(3)_c \times SU(2)_L \times U(1)_Y$ gauge symmetry.

1.4 The Drell-Yan process

Due to its importance in this thesis for the search for heavy resonances in the dielectron final state (see Chapter **??**), the Drell-Yan (DY) [6] process is introduced with more details. The DY process is defined as the annihilation of a quark-antiquark pair into a pair of oppositely-charged leptons. The Feynman diagrams of the DY process at leading order are shown in Figure 1.3.

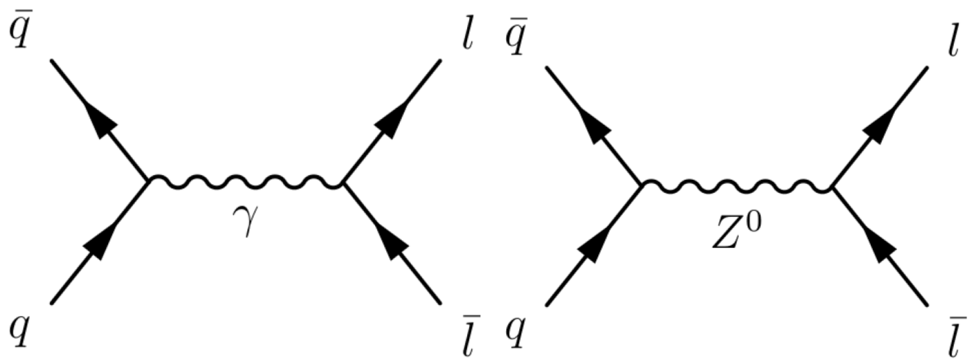

Figure 1.3: Feynman diagrams contributing to the Drell-Yan process at leading order. The left (right) diagram corresponds to the annihilation of a $q\bar{q}$ pair into a photon (a Z boson).

The diagram in Figure 1.4, with a Higgs boson exchange is neglected. Indeed, the coupling between the fermion and the Higgs boson is proportional to m_{f}/v, where m_{f} is the mass of the fermion and v is the vacuum expected value of the scalar field (≈ 246 GeV). So the amplitude of this diagram is proportional to $\frac{m_{\mathrm{q}}(\mathrm{GeV})}{246} \cdot \frac{m_{\ell}(\mathrm{GeV})}{246}$ with m_{ℓ} be the mass of lepton. As we know, the valence quarks in the proton are the up and down quarks which are light ($m < 10$ MeV). Therefore the contribution of the third diagram is several orders of magnitude smaller than the first two diagrams in proton proton collision and it is usually neglected in the calculation.

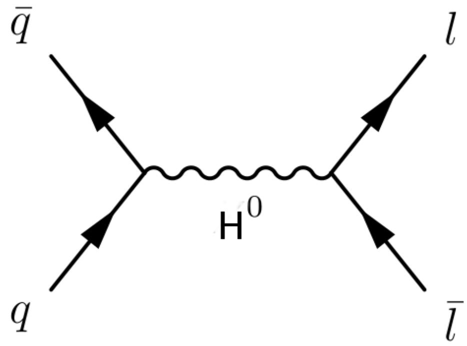

Figure 1.4: Feynman diagram of the process $\mathrm{q} + \bar{\mathrm{q}} \to \mathrm{H}^0 \to \ell + \bar{\ell}$ at leading order.

Cross-section

The diagrams in Figure 1.3 give rise to two matrice terms $\mathcal{M}_{\gamma}$ and $\mathcal{M}_{\mathrm{Z}}$, hence the cross section of DY process can be expressed as:

$$\sigma_{\gamma/\mathrm{Z}} = \sigma_{\gamma} + \sigma_{\mathrm{Z}} + \sigma_{int} \tag{1.21}$$

where σ_γ is the cross-section corresponding to the exchange of a photon only, σ_Z is for the exchange of a Z boson only, and σ_{int} is the cross-section from the interference of the first two processes.

The formulas in the rest of the section are taken from [62].

To be specific, the Equation 1.21 can be written as:

$$\sigma(q(p_1)\bar{q}(p_2) \to l^+l^-) = \frac{4\pi\alpha^2}{3s}\frac{1}{N}(Q_q^2 - 2Q_qV_lV_q\chi_1(s) + (A_l^2 + V_l^2)(A_q^2 + V_q^2)\chi_2(s)) \tag{1.22}$$

with

$$\chi_1(s) = \kappa\frac{s(s - M_Z^2)}{(s - M_Z^2)^2 + \Gamma_Z^2 M_Z^2}$$
$$\chi_2(s) = \kappa^2\frac{s^2}{(s - M_Z^2)^2 + \Gamma_Z^2 M_Z^2}$$
$$\kappa = \frac{\sqrt{2}G_F M_Z^2}{16\pi\alpha}$$

Here p_1 is the four-momenta of the quark, p_2 is the four-momenta of the anti-quark, and $s = (p_1 + p_2)^2$. The α is the electromagnetic coupling, the G_F is the Fermi constant with the value 1.1663787×10^{-5} GeV^{-2} [63], which can be precisely determined by muon lifetime experiment. The M_Z and Γ_Z are the mass and total decay width of the Z boson respectively. The $\frac{1}{N} = \frac{1}{3}$ and it is due to the color matching between quark and anti-quark. The Q_q is the charge of the quark, the V and A are the vectorial and axial couplings associated to the lepton/quark. The value of V and A are

$$V_f = T_f^3 - 2Q_f\sin^2\theta_W, \qquad A_f = T_f^3$$

with ${T_f}^3 = +\frac{1}{2}$ for $f = \nu, u, ...$ and ${T_f}^3 = -\frac{1}{2}$ for $f = e, d, ...$ The θ_W in $\sin^2\theta_W$ is so called "weak mixing angle" and it has been mathematically defined as $\cos\theta_W = \frac{M_W}{M_Z}$, here the M_W is the mass of W boson.

The first term ($\frac{4\pi\alpha^2}{3s}\frac{1}{N}Q_q^2$) in the right side of Equation 1.22 is corresponding to σ_γ and it can be calculated using QED. The second term ($\frac{4\pi\alpha^2}{3s}\frac{1}{N}(-2Q_qV_lV_q\chi_1)$) is for σ_{int} and the last term ($\frac{4\pi\alpha^2}{3s}\frac{1}{N}(A_l^2 + V_l^2)(A_q^2 + V_q^2)\chi_2$) is for σ_Z.

From Equation 1.22 one can see that at low centra-mass of energy ($\sqrt{s}$) the Drell-Yan cross section is dominated by photon exchange process (e.g. at $\sqrt{s} = M_Z/2$, the σ_γ is around 100 times greater than σ_Z and over 10 times larger than σ_{int}), while at Z pole ($\sqrt{s} \sim M_Z$) it is dominated by Z boson exchange process (e.g. at $\sqrt{s} = M_Z$, the σ_Z is well over 100 times larger than σ_γ, while σ_{int} is zero). To get a feeling about the Drell-Yan cross section as the function of lepton pair mass M_{ll} one can see Figure 1.5.

1.5 The photon induced process

As we known, the production of high invariant mass opposite sign lepton pairs in proton proton collision at the LHC is dominated by the Drell-Yan process (See previous section). Addition to this, photon-photon collisions, where the photons are radiated by the quarks in the proton, can also produce lepton pairs. The Feynman diagrams for the photon induced (PI) production of lepton pairs at leading order can be seen in Figure 1.6. The left diagram corresponds to a t-channel process and the right diagram corresponds to a u-channel process. There is no s-channel for the PI process at leading order and this will give different kinematic properties for the lepton pair comparing with Drell-Yan process which is s-channel.

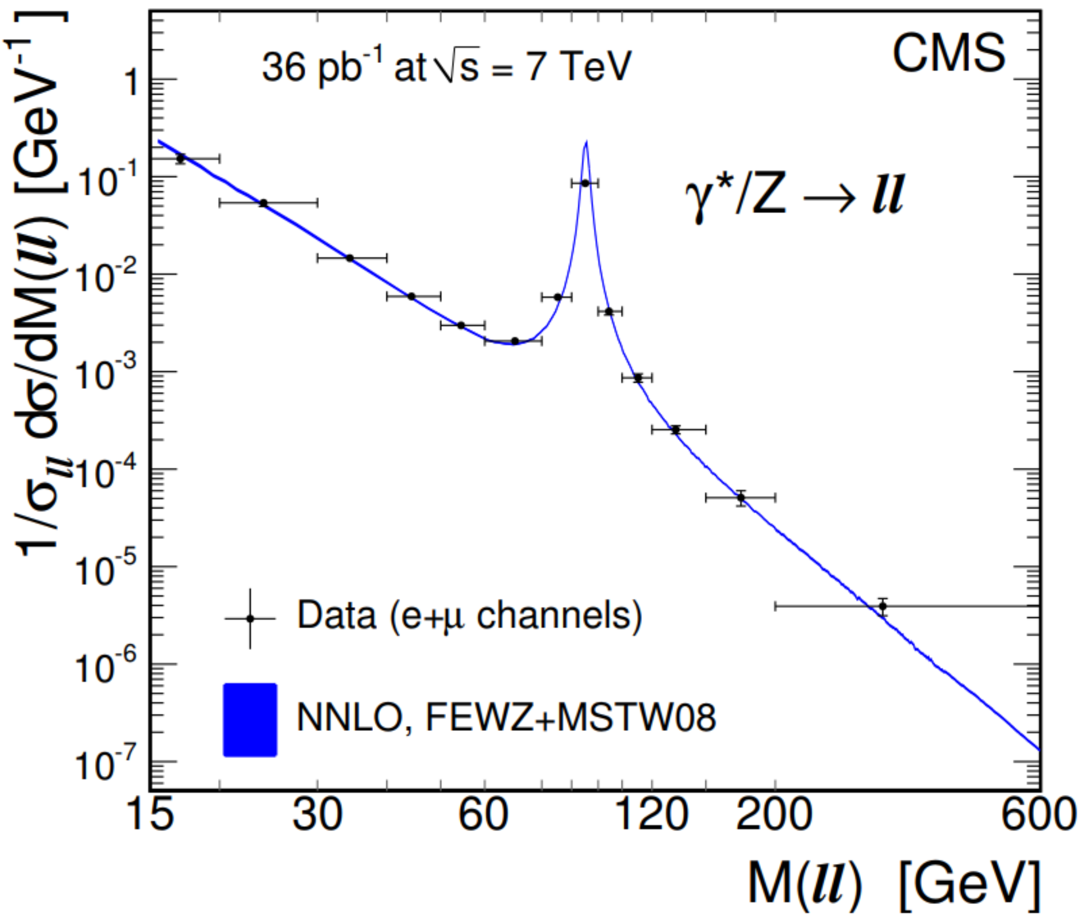

Figure 1.5: The normalized (in Z resonance region) DY cross section as the function of lepton pair mass (M_{ll}) in pp collision at $\sqrt{s} = 7$ TeV with CMS data [64].

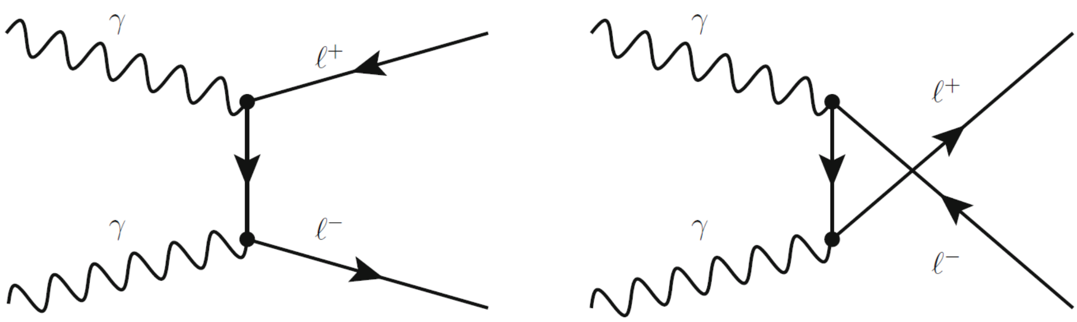

Figure 1.6: Feynman diagrams for the photon induced production of lepton pairs at leading order. The left (right) diagram corresponds to a t-channel (u-channel) process.

The contribution from PI process becomes a significant part of the dilepton production at high invariant masses. Therefore, the knowledge of this process is important input for high mass resonant (like Z') or non-resonant searches. From [65] we know the PI effects are generally small, not above the 5% level, for masses of up to $\sim$ 2 TeV, but can reach $\sim$ 15 - 20% above 5 TeV. This effects will be taken into account in searching for Z' study in Chapter **??**.

1.6 The effective field theory

If new physics scale is reachable at the experiment then the new physics could be directly observed via the production of new particles. Otherwise, it can take part in as a virtual particle which can not be detected directly but can still have an impact on the SM interactions by modifications of SM couplings or enhancements of rare SM processes. In the latter case, the effective field theory (EFT) approach is useful to parameterize and constrain new physics. In EFT, we extend the SM by adding new terms to the Lagrangian. An example of the extended Lagrangian is shown in Equation 1.23 where Λ represents the energy scale beyond which new physics becomes relevant, $\mathcal{C}_i$ stands for the dimensionless Wilson coefficients (also called as the effective couplings), $\mathcal{O}_i^6$ are dimension-six operators. Therefore, the underlying new physics particle gets integrated out (by measuring only $\mathcal{C}_i/\Lambda^2$) and leaving only the effective vertex, such as the Fermi theory for neutron decay (see the Feynman diagram in Figure 1.7). Besides, the EFT must maintain all the necessary symmetries of the SM. There are total O(100) new EFT vertices and it can be reduced by focusing on specific physical processes.

$$\mathcal{L} = \mathcal{L}_{SM} + \sum_i \frac{\mathcal{C}_i}{\Lambda^2}\mathcal{O}_i^6 \tag{1.23}$$

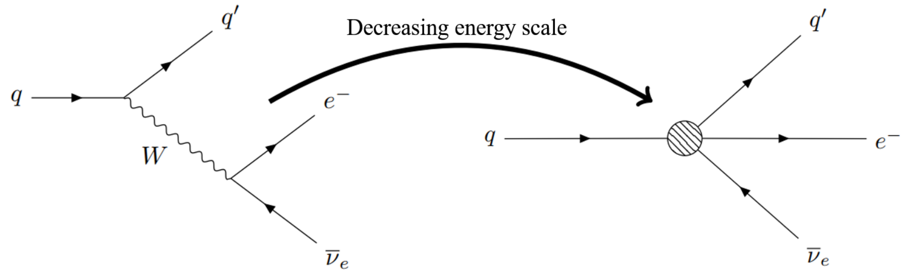

Figure 1.7: The Feynman diagram for neutron decay for high energy scale (left) and low energy scale (right).

The EFT provides an important and powerful technique for searching for areas of new physics and it has the following properties:

1. It is a model independent approach, which means it does not depend on whatever the underlying new physics is. Therefore, it allows a systematically search for new physics in SM processes;
2. It is able to impose the same strict symmetry requirements as in the SM;
3. It can recover the full SM theory in a very natural way;
4. It can be used to quantify the accuracy with which new physics can be excluded.

In this thesis the EFT approach is used for searching for new physics in top production which is reported in Chapter **??**.

1.7 Summary

In this chapter, an introduction of the SM is delivered including the descriptions of the elementary particles and the three fundamental forces (electromagnetic, weak and strong). After that, a brief description about gauge symmetry is given. Due to its importance in this thesis, the Drell-Yan process is also introduced. Moreover, the photon induced dilepton production process is shortly discussed. Finally, a basic introduction about the effective field theory is given.

Chapter 2

The beyond Standard Model of particle physics

This Chapter describes the motivations for new theories beyond the Standard Model (BSM) in Section 2.1 and introduces some BSM theories that predict the existence of heavy resonances which can decay to a dilepton final state [1] in Section 2.2. Finally, an introduction to the search for new physics in top quark production is given in Section 2.3.

2.1 Motivation for new physics

Despite the tremendous success of SM, there are still some shortcomings about it. Such as the existence of neutrino mass [9, 10], the existence of dark matter and dark energy [7, 8] and the matter-antimatter asymmetry. All of these observations can not be explained by SM. Besides, there are some limitations for the SM, such as lack of gravity description, convergence of the coupling constants [66]. Finally, the hierarchy problem and the existence of large number of free parameters in SM [53] make it looks unnatural. Therefore, it is commonly admitted that the SM is an effective model of a more fundamental theory at high energy. Each of these issues is shortly described in below.

- **Neutrino mass:** In the SM, the neutrino is assumed to be massless. However, it is observed that neutrinos can change from one flavour to another flavour which implies that they must have non-zero mass differences [9, 10] and their mass eigenstates are different from their flavour eigenstates. Experimentally, only upper limits on the neutrino masses have been set ($m < 2$ eV [53]). In addition, the differences between the neutrino squared masses have been measured: $\Delta m^2_{12} = (7.53 \pm 0.18) \times 10^{-5}$ eV^2 and $\Delta m^2_{32} = (2.44 \pm 0.06) \times 10^{-3}$ eV^2 [67].
- **Dark matter and dark energy:** Some astronomical observations show that the visible content of matter is only be $\sim 5\%$ of the total matter and energy content of the universe. Firstly, it is measured that the orbital velocities of stars around their galaxy center are too fast [7, 8] which is incompatible with the observed matter density in space. In order to solve the conflict between the experimental result and the theory prediction, the existence of "dark" matter which does not interact via electromagnetic or strong interaction has been proposed. Secondly, it is discovered that the universe is in accelerated expansion which means the galaxies are recede from each other and their escape rate increases with the distance [68, 69]. Giving these two cosmological

1. In this thesis, the expression "dilepton final state" denotes the decay in electron-positron pair (e^+e^-) or muon-antimuon pair ($\mu^+\mu^-$).

results, one can conclude that the matter (or energy) content of the universe is made of 5% ordinary matter, 25% dark matter and 70% dark energy which gives repellent force and is thought to be responsible for the observed accelerated expansion of the universe. However, the SM does not provides the candidates for dark matter as well as it can not explain the dark energy problem.

- **Asymmetry between matter and antimatter:** It is believed that matter and antimatter were produced with the same quantities at the time of Big Bang. However, we are living in a world composed with matter. So why does this happen and is it possible that some corners of the universe are dominated by antimatter? In 1967, Sakharov identified the three mechanisms necessary to obtain a global matter or antimatter asymmetry [70]:
  – Baryon and lepton number violation;
  – Interactions in the universe out of thermal equilibrium at a given moment of the universe history;
  – Charge (C) and charge-parity (CP) violation (the rate of a process $i \to f$ can be different from the CP conjugate process $\bar{i} \to \bar{f}$).

  The SM includes sources of CP violation: one is from a complex phase factor in the Cabibbo-Kobayashi-Maskawa (CKM) [71, 72] unitary matrix (which contains information on the strength of the flavour-changing weak interaction), and the other in the form of the QCD vacuum angle, θ_{QCD} [73]. However, they are not sufficient to explain the magnitude of the observed matter-antimatter asymmetry.
- **Free parameters of the SM:** There are 19 free parameters which have to be measured in the SM. The parameters include the masses of charged lepton, the masses of quark, the coupling constants of the three forces, the mass and vacuum expectation value of the Higgs boson, the mixing angles and the CP violating phase of the CKM matrix [2]. Due to this large number of free parameters, it is widely believed that there could be a more general and elegant theory than the SM. The list of parameters is summarized in Table 2.1.
- **Gravitational interaction and hierarchy problem:** The gravity, the fourth fundamental interaction, is not included in the SM because of its very small interaction strength compared with other three forces. The electromagnetic, weak and strong forces have similar strengths at the electroweak scale (energies of $\approx$ 100 GeV), but gravity is more than 10^{30} times weaker. The energy at which gravitational interactions becomes relevant is at the order of the Planck scale of $E_{Pl} = 10^{19}$ GeV, which is defined by the Planck mass, $M_{Pl} = \sqrt{\hbar c/G}$, where G is the gravitational constant. The huge difference between the electroweak scale and the Planck scale is also known as the hierarchy problem and it is deeply connected to the problem of the Higgs boson mass fine-tuning (which is expressed in the following).
- **Fine-tuning of the Higgs boson mass:** All the ingredients of the SM have been experimentally established after the discovery of the Higgs boson and the measurement of its mass ($\approx$ 125 GeV). All particles in the SM have a *bare mass* which is the mass obtained from the quantum propagator at the lowest order in perturbation theory. This is can be different from *physical mass* which contains higher order loop radiative corrections and can be measured in experiment.

  It is known [75] that the squared Higgs physical mass (m_{H}) can be obtained by the squared bare mass (m_0) of Higgs corrected with an extra term which includes higher order corrections (δm_{H}^2):

$$m_{\mathrm{H}}^2 = m_0^2 - \delta m_{\mathrm{H}}^2 \tag{2.1}$$

2. In addition, there are 7 parameters come from neutrino section: 3 neutrino masses, 3 mixing angles between different neutrinos, and 1 CP violating phase.

Quantity	Symbol	Value
Electron mass	m_{e}	511 keV
Muon mass	m_{μ}	105.7 MeV
Tau mass	m_{τ}	1.78 GeV
Up quak mass	m_{u}	2.3 MeV ($\mu_{\overline{\mathrm{MS}}}$=2 GeV)
Down quak mass	m_{d}	4.8 MeV ($\mu_{\overline{\mathrm{MS}}}$=2 GeV)
Strange quak mass	m_{s}	95 MeV ($\mu_{\overline{\mathrm{MS}}}$=2 GeV)
Charm quak mass	m_{c}	1.28 GeV ($\mu_{\overline{\mathrm{MS}}} = m_{\mathrm{s}}$)
Bottom quak mass	m_{b}	4.18 GeV ($\mu_{\overline{\mathrm{MS}}} = m_{\mathrm{b}}$)
Top quak mass	m_{t}	173.5 GeV
W boson mass	m_{W}	80.4 GeV
Z boson mass	m_{Z}	91.2 GeV
Higgs boson mass	m_{H}	125.09 GeV [74]
Higgs boson vacuum expectation value	v	246 GeV
Strong coupling constant	α_s	0.119 ($\mu_{\overline{\mathrm{MS}}} = m_{\mathrm{Z}}$)
QCD vacuum angle	θ_{QCD}	~ 0
CKM 12-mixing angle	θ_{12}	12.9°
CKM 23-mixing angle	θ_{23}	2.4°
CKM 13-mixing angle	θ_{13}	0.2°
CKM CP violating phase	δ_{13}	69°

Table 2.1: The SM parameters. The quark masses are presented in the renormalization scheme known as $\overline{\mathrm{MS}}$ [53].

where δm_{H}^2 includes all contributions from radiative corrections to the Higgs propagator. The main contributions include the top quarks, the Higgs boson itself, and the vector bosons. The related Feynman diagrams are shown in Figure 2.1, where the Higgs boson is denoted as h [53].

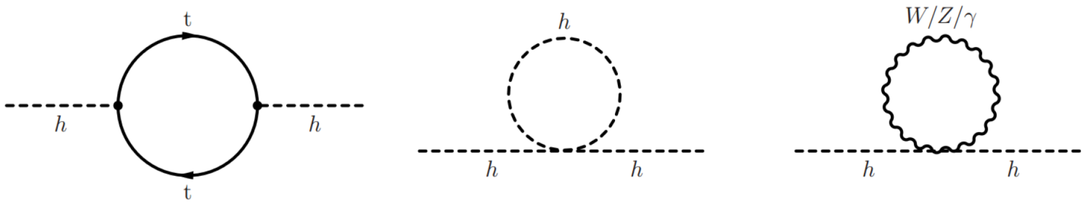

Figure 2.1: The Feynman diagrams of the processes which give the main divergent contributions to the Higgs boson mass.

However, the integrals corresponding to the amplitude of these processes are divergent, so a cut-off parameter Λ is introduced. The Λ represents the energy scale, up to which the SM is still valid. In principle, one can assume that the SM is valid up to the Planck scale at which gravitational effects cannot be neglected. With this assumption Λ would be of the order of $\approx 10^{19}$ GeV. The full calculation gives that δm_{H}^2 is proportional to Λ^2:

$$\delta m_{\mathrm{H}}^2 \propto \Lambda^2 \approx 10^{38}\ \mathrm{GeV}^2 \tag{2.2}$$

Because m_{H} is ≈ 125 ($\approx 10^2$) GeV, Equation (2.1) can be rewritten as:

$$10^4\ \mathrm{GeV}^2 \approx m_0^2 - \Lambda^2 \approx m_0^2 - 10^{38}\ \mathrm{GeV}^2$$

which means that m_0^2 is of the same order of Λ^2 (10^{38}) and these two terms cancel with a very high precision to obtain the value of the Higgs physical mass. This mathematical problem is called "Higgs mass fine-tuning" problem, although it does not invalidate the theory. However, it seems an unnatural and implausible coincidence that m_0^2 cancels all the loop contributions up to this astonishing precision.

Actually, the problem comes from the choice of the Λ. If we choose the Λ to be ≈ 1 TeV, then the problem is solved because the cancellation is of the order of one over ten which seems is a natural and acceptable value. For this reason, if one accepts the Higgs mass fine-tuning argument, then the new physics will appear at the TeV scale, because at energy higher than $\Lambda = 1$ TeV, the SM is not valid anymore.

- **Convergence of the coupling constants**: In SM, the coupling strengths for electromagnetic interaction, weak interaction, and strong interaction have a close value at the energy scale $\mathcal{O}(10^{16})$ GeV. However, these three coupling strengths can not converge at a single point which is shown in Figure 2.2. In order to unify these couplings, an extension of the SM is needed and the new physics will be involved.

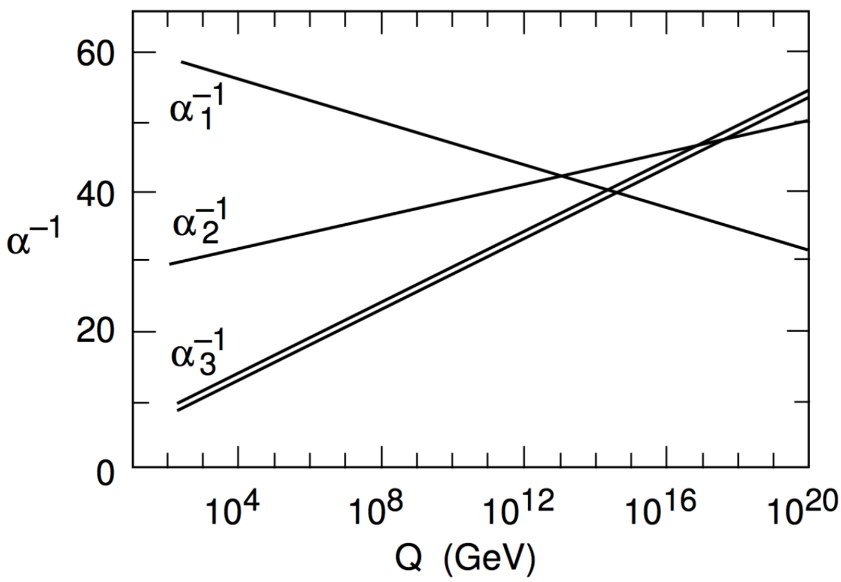

Figure 2.2: Evolution of the SM couplings $\alpha_i = \frac{g_i^2}{4\pi}$ as a function of the energy scale [66].

All these issues indicate that there must be new physics at a scale beyond the electroweak scale. Driven by the hierarchy problem, it is believed that there should be new physics at the TeV scale. Therefore, a discovery with direct searches at the Large Hadron Collider (LHC) could be possible.

2.2 New heavy particles decaying into a lepton pair

The most directly way to search for a new heavy particle decaying into a lepton pair would be searching for the "bump" (or localized excess) in dilepton mass spectrum at high mass. This study is motivated both theoretically and experimentally. From a theoretical point of view, many beyond SM (BSM) models predict the existence of new massive resonances which can decay into dilepton. Such as:

- The supersymmetric model [11] which is extremely attractive, because it can provide an explanation to the Higgs mass fine-tuning problem. In order to avoid issue of naturalness for the Higgs boson mass, the supersymmetric particles cannot be much heavier than 1 TeV which makes searching for these new particles is doable at LHC. Besides, the supersymmetric models provide a natural candidate of dark matter. There are many supersymmetric models, the simplest one is the Minimal Supersymmetric Standard Model (MSSM) where each SM particle has a superymmetric partner. The fermions have spin 0 "sfermion" partners, gauge bosons have spin $\frac{1}{2}$ "gaugino" partners and the super-partner for higgs is "higgsinos". In SM, the baryon (B) number and lepton (L) number are conserved, where $\mathrm{B} = \frac{1}{3}(\mathrm{n_q} - \mathrm{n_{\bar{q}}})$ and $\mathrm{L} = (\mathrm{n_l} - \mathrm{n_{\bar{l}}})$. However, in the MSSM the B and L can be violated. In order to maintain the experimentally verified conservation laws, one defines a new conserved quantum number, the R-parity $\mathrm{P_R}$ as:

$$\mathrm{P_R} = (-1)^{3\mathrm{B}-\mathrm{L}+2\mathrm{s}},$$

where s is the spin of the particle. For the SM particles the $\mathrm{P_R} = +1$ and for supersymmetric particles the $\mathrm{P_R} = -1$. Due to the conserved $\mathrm{P_R}$, the supersymmetric particles can not decay into dilepton final states. However, in more complicated supersymmetric model [76] where the $\mathrm{P_R}$ can be violated, the new particles (e.g. "sneutrinos") can decay into dilepton final states.

- The Grand Unified Theory (GUT) [12, 13, 14] which tries to unify electromagnetic, weak, and strong interactions into one interaction through the extensions of the SM gauge group is also attractive. There are many GUT models, the starting point is the $SU(5)$ [77] model which was initially proposed by Georgi and Glashow in 1974. $SU(5)$ is the smallest gauge group that can contain the SM (can be expressed by $SU(5) \supset SU(3)_c \times SU(2)_L \times U(1)_Y$). It supposes the coupling strengths of electromagnetic (g_1), weak (g_2), and strong (g_3) interactions will merge into a single coupling (g_G) at the energy scale $\mathcal{O}(10^{16})$ GeV (which is called the unification scale). Besides, it predicts the $\sin^2\theta_\mathrm{W} = 0.375$ at the unification scale, and this was compatible with the measurements at that time. However, the $\sin^2\theta_\mathrm{W} = 0.375$ is now ruled out by most precise measurements and consequently g_1, g_2 and g_3 do not converge at single point. Moreover, in $SU(5)$ the decay of proton is allowed (e.g. $p \to e^+ + \pi^0$), while the predicted half time of the proton decay is several orders of magnitude smaller than the experimental lower limits. Therefore, it seems the simplest $SU(5)$ is not a correct GUT model.

  Another famous GUT model is $SO(10)$ [78] which was proposed by H. Fritzsch and P. Minkowski in 1975. In $SO(10)$ all matter particles belonging to the same generation are grouped into a single multiplet and has the nice feature to predict an half time for the proton decay which is not in contradiction with the experimental results. In $SO(10)$, the symmetries can be broken at different scale. For instance, the breaking scheme for $SO(10)$ could be:

$$SO(10) \to SU(5) \times U(1)_\chi \to G_{SM} \times U(1)_\chi$$

  where G_{SM} is $SU(3)_c \times SU(2)_L \times U(1)_Y$ and χ is the charge associated to the extra $U(1)_\chi$ group. There is no constraint on the breaking scale for this $U(1)_\chi$ and it might happen at the TeV scale.

  Moreover, the E_6 model [79] is also popular which is able to embed $SU(5)$ lie on the exceptional E_6 group. The E_6 group can break down to SM by following scheme:

$$E_6 \to SO(10) \times U(1)_\psi \to SU(5) \times U(1)_\chi \times U(1)_\psi \to G_{SM} \times U(1)_\chi \times U(1)_\psi.$$

  The new particle Z' from the linear combination of $U(1)_\chi$ and $U(1)_\psi$ is given by:

$$\mathrm{Z}' = \mathrm{Z}'_\psi \cos\theta_{\mathrm{E_6}} + \mathrm{Z}'_\chi \sin\theta_{\mathrm{E_6}}$$

  where $0 \le \theta_{\mathrm{E_6}} \le \pi$ is a mixing angle. Therefore, different $\theta_{\mathrm{E_6}}$ will give different Z'.

Some specific $Z^{'}$s are: 1, the $Z^{'}{}_{\psi}$ ($\theta_{E_6} = 0$) that only interacts through axial-vector couplings with the fermions and it is predicted by superstring theories [80]. 2, the $Z^{'}{}_{\chi}$ ($\theta_{E_6} = -\frac{\pi}{2}$) that corresponds to a pure $U(1)_{\chi}$ group. 3, the $Z^{'}{}_{\eta}$ ($\theta_{E_6} = \arccos\sqrt{\frac{5}{8}}$), also suggested by superstring theories [80]. 4, the $Z^{'}{}_{I}$ (θ_{E_6}=(arccos$\sqrt{\frac{5}{8}}$)-$\frac{\pi}{2}$) that does not couple to up quarks and only couples to left-handed down quarks and right-handed leptons. The couplings between these specific $Z^{'}$s and the up quarks, the down quarks, and the charged leptons can be seen in Table 2.2.

Last but not least, the Sequential Standard Model (SSM) [12] $Z^{'}$ has couplings which are exactly the same as those of the SM Z (see Table 2.2), but is just heavier. This is not a real model but is very commonly used as a "standard candle" in experimental $Z^{'}$ (or $W^{'}$) searches.

Model	θ_{E_6}	c_V^u	c_A^u	c_V^d	c_A^d	c_V^l	c_A^l
$Z^{'}{}_{\psi}$	0	0	0.301	0	0.301	0	0.301
$Z^{'}{}_{\eta}$	$\arccos\sqrt{\frac{5}{8}}$	0	0.380	-0.285	0.0950	0.285	0.0950
$Z^{'}{}_{\chi}$	$-\frac{\pi}{2}$	0	0.0735	-0.416	-0.343	0.416	-0.343
$Z^{'}{}_{I}$	$(\arccos\sqrt{\frac{5}{8}})-\frac{\pi}{2}$	0	0	0.621	-0.621	-0.621	-0.621
$Z^{'}{}_{SSM}$	–	-0.227	0.593	0.410	-0.593	0.0446	-0.593

Table 2.2: The specific $Z^{'}$ bosons with corresponding θ_{E_6} form E_6 model together with the vector (c_V) and axial (c_A) couplings between the $Z^{'}$ and the up quarks (u), the down quarks (d), and the charged leptons (l). The $Z^{'}{}_{SSM}$ from the Sequential Standard Model which has the same SM couplings is also shown.

- In order to explain the large difference between the electroweak scale ($\mathcal{O}(100)$ GeV) and the Planck scale ($\mathcal{O}(10^{19})$ GeV), the theories involve extra dimensions are proposed. It is assumed that there exist a spin 2 graviton (the carrier of the gravitational interaction and can decay into dielectron or dimuon pair) that can propagate in extra dimensions which have small radius R (R should be less than 100 μm [81] and assuming all the extra dimensions share the same radius), while SM forces are confined in usual 4-dimension spacetime. Due to the overlap of the wave functions of the SM particles with the graviton is small in 4-dimension spacetime, the gravity is much weaker than other three forces in our 4-dimension world. There are many extra dimensions models, such as ADD model (proposed by Arkani-Hamed, Dimopulous and Dvali) [15] which is one of the first solutions of the hierarchy problem by involving extra spatial dimensions. In ADD model, the R decreases with the increases of the number of extra dimension n. For $n = 1$, the R is around 10^{11} m at which distances the Newton's law is well established. However, the prediction from ADD for $n = 1$ gives deviations to the one from Newton's law. Therefore, $n = 1$ is excluded in ADD and n should start from 2 which corresponds to $R = 100$ μm which is just at the experimental limits [81]. Another type of extra dimension model using 5-dimensional warped geometry theory has been developed by Randall and Sundrum [16] called "Randall-Sundrum model". The Randall-Sundrum model uses "brane"[3] to describe SM particles ("Weakbrane") and graviton ("Planckbrane"), and gravity is much weaker on the Weakbrane than on the Planckbrane.

Generically, the spin 1 particle that can give rise to a resonance in the dilepton mass spectrum is called $Z^{'}$, while for spin 2 particle it is called "graviton".

3. A brane is a physical object that generalizes the notion of a point particle to higher dimensions

From an experimental point of view, these BSM models of new physics give rise to high energy lepton pair in the final states and the SM background for such final states is relatively low at a hadron collider. Searches for heavy resonance decaying into dilepton have been performed at LHC and Tevatron. The CMS Collaboration at the LHC performed the search with proton-proton collision data collected at $\sqrt{s} = 7$ TeV [26, 27], with data collected at 8 TeV [28, 29], and using the combination of 2015 data collected at 13 TeV with data collected at 8 TeV [30]. Recently, CMS performed this search using the data collected at 13 TeV from 2016 [31] and 2017 [32], this search will be presented in detail in Chapter **??**. Similar to CMS, the ATLAS Collaboration also performed the search with data collected at 7 TeV [33, 34], with data collected at 8 TeV [35], and with data collected at 13 TeV [36, 37]. At the Tevatron, the CDF and D0 Collaborations have published results based on a $\mathrm{p}-\bar{\mathrm{p}}$ collision sample at $\sqrt{s} = 1.96$ TeV, corresponding to an integrated luminosity of approximately 5 fb^{-1} [38, 39, 40, 41, 42, 43].

2.3 New physics in top quark production

As described in Section 2.2 if the new physics scale is available at hadron collider, the existence of new physics could be directly observed via the production of new particles. Otherwise, new physics could affect SM interactions indirectly, through modifications of SM couplings or enhancements of rare SM processes. In the latter case, it is useful to introduce a model-independent approach to parameterize and to constrain possible deviations from SM predictions, independently of the fundamental theory of new physics.

Due to its large mass, close to the electroweak symmetry breaking scale, the top quark is expected to play an important role in several new physics scenarios. An effective field theory (EFT) (See Section 1.6) approach is followed in this thesis to search for new physics in the top quark sector in the ee and $\mu\mu$ final states (the experimental setup and results are shown in Chapter **??**). In Refs. [82, 83] all dimension-six operators that contribute to the top quark pair production ($\mathrm{t\bar{t}}$) and the single top quark production in association with a W boson (tW) are investigated. The operators and the related effective Lagrangian, which are relevant for dilepton final states, can be written as [84]:

$$\mathrm{O}_{\phi q}^{(3)} = (\phi^{+}\tau^{I}\mathrm{D}_{\mu}\phi)(\bar{q}\gamma^{\mu}\tau^{I}q), \quad L_{eff} = \frac{\mathrm{C}_{\phi q}^{(3)}}{\sqrt{2}\Lambda^{2}} g v^{2}\bar{b}\gamma^{\mu}\mathrm{P_L} t \mathrm{W}_{\mu}^{-} + \mathrm{h.c.}, \tag{2.3}$$

$$\mathrm{O}_{\mathrm{tW}} = (\bar{q}\sigma^{\mu\nu}\tau^{I}t)\tilde{\phi}\mathrm{W}_{\mu\nu}^{I}, \quad L_{eff} = -2\frac{\mathrm{C}_{\mathrm{tW}}}{\Lambda^{2}} v\bar{b}\sigma^{\mu\nu}\mathrm{P_R} t\partial_{\nu}\mathrm{W}_{\mu}^{-} + \mathrm{h.c.}, \tag{2.4}$$

$$\mathrm{O}_{\mathrm{tG}} = (\bar{q}\sigma^{\mu\nu}\lambda^{A}t)\tilde{\phi}\mathrm{G}_{\mu\nu}^{A}, \quad L_{eff} = \frac{\mathrm{C}_{\mathrm{tG}}}{\sqrt{2}\Lambda^{2}} v\left(\bar{t}\sigma^{\mu\nu}\lambda^{A}t\right)\mathrm{G}_{\mu\nu}^{A} + \mathrm{h.c.}, \tag{2.5}$$

$$\mathrm{O}_{\mathrm{G}} = f_{ABC}\mathrm{G}_{\mu}^{A\nu}\mathrm{G}_{\nu}^{B\rho}\mathrm{G}_{\rho}^{C\mu}, \quad L_{eff} = \frac{\mathrm{C}_{\mathrm{G}}}{\Lambda^{2}} f_{ABC}\mathrm{G}_{\mu}^{A\nu}\mathrm{G}_{\nu}^{B\rho}\mathrm{G}_{\rho}^{C\mu} + \mathrm{h.c.}, \tag{2.6}$$

$$\mathrm{O}_{\mathrm{u(c)G}} = (\bar{q}\sigma^{\mu\nu}\lambda^{A}t)\tilde{\phi}\mathrm{G}_{\mu\nu}^{A}, \quad L_{eff} = \frac{\mathrm{C}_{\mathrm{u(c)G}}}{\sqrt{2}\Lambda^{2}} v\left(\bar{u}\left(\bar{c}\right)\sigma^{\mu\nu}\lambda^{A}t\right)\mathrm{G}_{\mu\nu}^{A} + \mathrm{h.c.}, \tag{2.7}$$

where $\mathrm{C}_{\phi q}^{(3)}$ (ϕ is Higgs field, q is quark), $\mathrm{C_{tW}}$, $\mathrm{C_{tG}}$, $\mathrm{C_G}$ and $\mathrm{C_{u(c)G}}$ stand for the dimensionless Wilson coefficients, also called effective couplings. The variable Λ represents the energy scale beyond which new physics becomes relevant. The detailed description of the operators is given in Refs. [82, 83]. The operators $\mathrm{O}_{\phi q}^{(3)}$ and $\mathrm{O_{tW}}$ modify the SM interaction between W boson, top quark, and b quark (Wtb). The triple gluon field strength operator $\mathrm{O_G}$ represents the only genuinely gluonic CP conserving term which can appear at dimension 6 within an effective strong interaction Lagrangian [85]. The operators $\mathrm{O_{uG}}$ and $\mathrm{O_{cG}}$

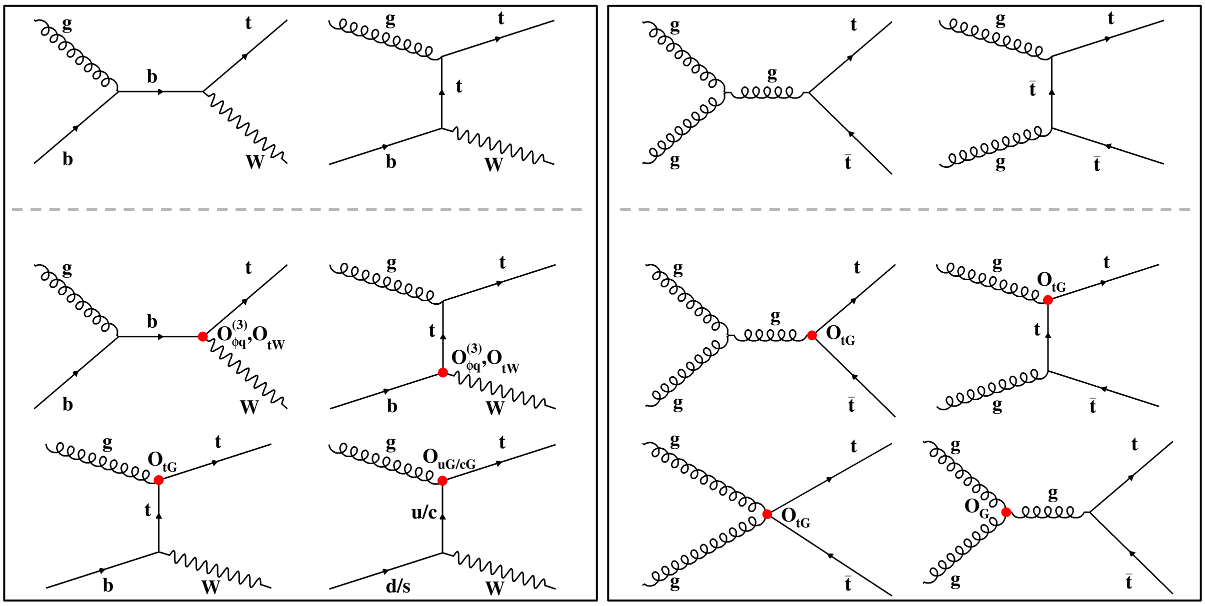

Figure 2.3: Representative Feynman diagrams for the tW (left panel) and $t\bar{t}$ (right panel) production at leading order. The upper row gives the SM diagrams, the middle and lower rows present diagrams corresponding to the $O^{(3)}_{\phi q}$, O_{tW}, O_{tG}, O_G, and $O_{u(c)G}$ contributions.

lead to flavor changing neutral current (FCNC) interactions of top quark and contribute to the tW production. As we know the FCNC processes do not exist at tree level in the SM and are induced only at loop level. Therefore the rates of FCNC processes are highly suppressed. The observation of such processes will be very important for searching new physics. The effect of introducing the new couplings $C^{(3)}_{\phi q}$, C_{tW}, C_{tG} and $C_{u(c)G}$ can be investigated in the tW production. The C_{tG} affects also the $t\bar{t}$ production. In the case of the C_G coupling, only the $t\bar{t}$ production is modified. It should be noted that the O_{tW} and O_{tG} operators with imaginary coefficient lead to CP-violating effects. Representative Feynman diagrams for new physics contributions in the tW and $t\bar{t}$ production are shown in Figure 2.3. In this analysis we only probe CP-even dimension six operators via top quark production.

Several searches for new physics in the top quark sector including new non-SM couplings have been performed at the Tevatron and LHC colliders. Results can be interpreted in two ways. Most of the previous analyses followed the anomalous coupling approach in which SM interactions are extended for possible new interactions. In this study, the EFT framework with effective couplings is used for the interpretation of the results. Constraints obtained on anomalous couplings can be translated to effective coupling bounds [82, 48]. A variety of limits have been set on the Wtb anomalous coupling through single top quark *t*-channel production and measurements of the W boson polarisation from top quark decay by the D0 [48], ATLAS [46, 47] and CMS [44, 45] Collaborations. Direct limits on the top chromomagnetic dipole moment have been obtained by the CMS Collaboration at 7 TeV using top quark pair events [86]. Searches for top quark FCNC interactions have been performed at Tevatron [50, 51] and at LHC [44, 49] via single top quark production and limits are set on related anomalous couplings.

2.4 Summary

In this chapter the shortcomings of SM and motivations of BSM are delivered. After that some BSM theories which predict the existence of heavy resonances decaying into dilepton are introduced. Finally, an indirect search for new physics through top production is described.

Acronym table

ALICE	A Large Ion Collider Experiment
ATLAS	A Toroidal LHC ApparatuS
CL	Confidence Level
CMS	Compact Muon Solenoid
CP	Charge Parity
CR	Color Reconnection
CSV	Combined Secondary Vertex
CSVv2	Combined Secondary Vertex version 2
DY	Drell-Yan
ECAL	Electromagnetic Calorimeter
EFT	Effective Field Theory
FCNC	Flavor Changing Neutral Current
FSR	Final State Radiation
GUT	Grand Unified Theory
HCAL	Hadronic Calorimeter
ISR	Initial State Radiation
JEC	Jet Energy Correction
JER	Jet Energy Resolution
LHC	Large Hadron Collider
LHCb	Large Hadron Collider beauty
MC	Monte Carlo
ME	Matrix Elements
MET	Missing Transverse Energy
MLP	Multiple Layer Perceptron
MVA	Multivariate Analysis
NLO	Next-Leading Order
NN	Neural Network
NNLO	Next-Next-Leading Order
PAG	Physics Analysis Group
PDF	Parton Distribution Function
PF	Particle-Flow
POG	Physics Object Group
PS	Parton Shower
PU	Pile Up
SM	Standard Model
SSM	Sequential Standard Model
UE	Underlying Event

Appendices

Bibliography

[1] David Griffiths. “Introduction to elementary particles”. In: (1987).

[2] Alan D. Martin Francis Halzen. “QUARKS AND LEPTONS: An Introductory Course in Modern Particle Physics”. In: (1984).

[3] S.N. Mukherjee T. Morii C.S. Lim. “The Physics of the Standard Model and Beyond”. In: (2004).

[4] The ATLAS Collaboration. “Observation of a new particle in the search for the Standard Model Higgs boson with the ATLAS detector at the LHC”. In: *Phys. Lett.* B716 (2012), pp. 1–29. DOI: 10.1016/j.physletb.2012.08.020. arXiv:1207.7214 [hep-ex].

[5] The CMS Collaboration. “Observation of a new boson at a mass of 125 GeV with the CMS experiment at the LHC”. In: *Phys. Lett.* B716 (2012), pp. 30–61. DOI: 10.1016/j.physletb.2012.08.021. arXiv:1207.7235 [hep-ex].

[6] Sidney D Drell and Tung-Mow Yan. “Partons and their applications at high energies”. In: *Annals of Physics* 66.2 (1971), pp. 578 –623. ISSN: 0003-4916. DOI: https://doi.org/10.1016/0003-4916(71)90071-6. URL: http://www.sciencedirect.com/science/article/pii/0003491671900716.

[7] Vera C. Rubin and W. Kent Ford Jr. “Rotation of the Andromeda Nebula from a Spectroscopic Survey of Emission Regions”. In: *Astrophys. J.* 159 (1970), pp. 379–403. DOI: 10.1086/150317.

[8] Katherine Freese. “Review of Observational Evidence for Dark Matter in the Universe and in upcoming searches for Dark Stars”. In: *EAS Publ. Ser.* 36 (2009), pp. 113–126. DOI: 10.1051/eas/0936016. arXiv:0812.4005 [astro-ph].

[9] Y. Fukuda et al. “Evidence for oscillation of atmospheric neutrinos”. In: *Phys. Rev. Lett.* 81 (1998), pp. 1562–1567. DOI: 10.1103/PhysRevLett.81.1562. arXiv:9807003 [hep-ex].

[10] Y. Abe et al. “Indication for the disappearance of reactor electron antineutrinos in the Double Chooz experiment”. In: *Phys. Rev. Lett.* 108 (2012), p. 131801. DOI: 10.1103/PhysRevLett.108.131801. arXiv:1112.6353 [hep-ex].

[11] R. Barbier et al. “R-parity violating supersymmetry”. In: *Phys.Rept.* 420 (2005). DOI: 10.1016/j.physrep.2005.08.006. arXiv:0406039 [hep-ex].

[12] G. Altarelli, B. Mele, and M. Ruiz-Altaba. “Searching for new heavy vector bosons in $p\bar{p}$ colliders”. In: *Z. Phys. C* 45 (1989), p. 109. DOI: 10.1007/BF01556677.

[13] A. Leike. “The Phenomenology of extra neutral gauge bosons”. In: *Phys.Rept.* 317 (1999), p. 143. DOI: 10.1016/S0370-1573(98)00133-1.

[14] J. L. Hewett and T. G. Rizzo. “Low-Energy Phenomenology of Superstring Inspired E(6) Models”. In: *Phys.Rept.* 183 (1989), p. 193. DOI: 10.1016/0370-1573(89)90071-9.

[15] N. Arkani-Hamed, S. Dimopoulos, and G. Dvali. “The hierarchy problem and new dimensions at a millimeter”. In: *Phys. Lett. B* 429 (1998), p. 263. DOI: 10.1016/S0370-2693(98)00466-3. arXiv:9803315 [hep-ph].

[16] L. Randall and R. Sundrum. “A Large mass hierarchy from a small extra dimension”. In: *Phys. Rev. Lett.* 83 (1999), p. 3370. DOI: 10.1103/PhysRevLett.83.3370.

[17] Battistoni et al. “The Application of the Monte Carlo Code FLUKA in Radiation Protection Studies for the Large Hadron Collider”. In: *Progress in Nuclear Science and Technology* 2 (Oct. 2011), pp. 358–364. DOI: 10.15669/pnst.2.358.

[18] CMS. “Public CMS Luminosity Information”. In: *CMS Twiki* https://twiki.cern.ch/twiki/bin/view/CMSPublic/LumiPublicResults ().

[19] Antonella Del Rosso. “HL-LHC updates in Japan. Projet HL-LHC : une r茅union fait le point au Japon”. In: BUL-NA-2014-272. 51/2014 (2014), p. 4. URL: https://cds.cern.ch/record/1975962.

[20] S. Chatrchyan et al. “The CMS Experiment at the CERN LHC”. In: *JINST* 3 (2008), S08004. DOI: 10.1088/1748-0221/3/08/S08004.

[21] CERN. “CERN website”. In: http://cms.web.cern.ch/news/cms-detector-design (2011).

[22] CERN. “CERN website”. In: http://cms.web.cern.ch/org/cms-presentations-public (2011).

[23] CMS Collboration. “CMS Physics: Technical Design Report Volume 1: Detector Performance and Software”. In: *Technical Design Report CMS. CERN, Geneva* http://cds.cern.ch/record/922757 (2016).

[24] CMS Collboration. “The Electromagnetic Calorimeter Technical Design Report”. In: *Technical Design Report CMS* http://cds.cern.ch/record/349375/files/ (1997).

[25] *The CMS hadron calorimeter project: Technical Design Report*. Technical Design Report CMS. The following files are from <a href=. Geneva: CERN, 1997. URL: http://cds.cern.ch/record/357153.

[26] Serguei Chatrchyan et al. “Search for resonances in the dilepton mass distribution in pp collisions at $\sqrt{s} = 7$ TeV”. In: *JHEP* 05 (2011), p. 093. DOI: 10.1007/JHEP05(2011)093. arXiv:1103.0981 [hep-ex].

[27] Serguei Chatrchyan et al. “Search for narrow resonances in dilepton mass spectra in pp collisions at $\sqrt{s} = 7$ TeV”. In: *Phys. Lett. B* 714 (2012), p. 158. DOI: 10.1016/j.physletb.2012.06.051. arXiv:1206.1849 [hep-ex].

[28] Serguei Chatrchyan et al. “Search for heavy narrow dilepton resonances in pp collisions at $\sqrt{s} = 7$ TeV and $\sqrt{s} = 8$ TeV”. In: *Phys. Lett. B* 720 (2013), p. 63. DOI: 10.1016/j.physletb.2013.02.003. arXiv:1212.6175 [hep-ex].

[29] Vardan Khachatryan et al. “Search for physics beyond the standard model in dilepton mass spectra in proton-proton collisions at $\sqrt{s} = 8$ TeV”. In: *JHEP* 04 (2015), p. 025. DOI: 10.1007/JHEP04(2015)025. arXiv:1412.6302 [hep-ex].

[30] The CMS Collaboration. “Search for narrow resonances in dilepton mass spectra in proton-proton collisions at $\sqrt{s} = 13$ TeV and combination with 8 TeV data”. In: *Phys. Lett.* B768 (2017), pp. 57–80. DOI: 10.1016/j.physletb.2017.02.010. arXiv:1609.05391 [hep-ex].

[31] The CMS Collaboration. “Search for high-mass resonances in dilepton final states in proton-proton collisions at $\sqrt{s} = 13$ TeV”. In: *Journal of High Energy Physics* 2018.6 (2018), p. 120. ISSN: 1029-8479. DOI: 10.1007/JHEP06(2018)120. URL: https://doi.org/10.1007/JHEP06(2018)120.

[32] The CMS Collaboration. “Search for high mass resonances in dielectron final state”. In: *CMS Physics Analysis Summaries* CMS-PAS-EXO-18-006 (2018).

[33] Georges Aad et al. “Search for high mass dilepton resonances in pp collisions at $\sqrt{s} = 7$ TeV with the ATLAS experiment”. In: *Phys. Lett. B* 700 (2011), p. 163. DOI: 10.1016/j.physletb.2011.04.044. arXiv:1103.6218 [hep-ex].

[34] Georges Aad et al. “Search for high-mass resonances decaying to dilepton final states in pp collisions at $\sqrt{s} = 7$ TeV with the ATLAS detector”. In: *JHEP* 11 (2012), p. 138. DOI: 10.1007/JHEP11(2012)138. arXiv:1209.2535 [hep-ex].

[35] Georges Aad et al. “Search for high-mass dilepton resonances in pp collisions at $\sqrt{s} = 8$ TeV with the ATLAS detector”. In: *Phys. Rev. D* 90 (2014), p. 052005. DOI: 10.1103/PhysRevD.90.052005. arXiv:1405.4123 [hep-ex].

[36] Morad Aaboud et al. “Search for new high-mass phenomena in the dilepton final state using 36.1 fb^{-1} of proton-proton collision data at $\sqrt{s} = 13$ TeV with the ATLAS detector”. In: *JHEP* 10 (2017), p. 182. DOI: 10.1007/JHEP10(2017)182. arXiv:1707.02424 [hep-ex].

[37] Georges Aad et al. “Search for high-mass dilepton resonances using 139 fb^{-1} of *pp* collision data collected at $\sqrt{s}$ =13 TeV with the ATLAS detector”. In: (2019). arXiv:1903.06248 [hep-ex].

[38] T. Aaltonen et al. “Search for high-mass e^+e^- resonances in $p\bar{p}$ collisions at $\sqrt{s} = 1.96$ TeV”. In: *Phys. Rev. Lett.* 102 (2009), p. 031801. DOI: 10.1103/PhysRevLett.102.031801. arXiv:0810.2059 [hep-ex].

[39] T. Aaltonen et al. “A search for high-mass resonances decaying to dimuons at CDF”. In: *Phys. Rev. Lett.* 102 (2009), p. 091805. DOI: 10.1103/PhysRevLett.102.091805. arXiv:0811.0053 [hep-ex].

[40] Victor Mukhamedovich Abazov et al. “Search for Randall–Sundrum gravitons in the dielectron and diphoton final states with 5.4 fb^{-1} of data from $\mathrm{p\bar{p}}$ collisions at $\sqrt{s} = 1.96$ TeV”. In: *Phys. Rev. Lett.* 104 (2010), p. 241802. DOI: 10.1103/PhysRevLett.104.241802. arXiv:1004.1826 [hep-ex].

[41] Victor Mukhamedovich Abazov et al. “Search for a heavy neutral gauge boson in the dielectron channel with 5.4 fb^{-1} of $\mathrm{p\bar{p}}$ collisions at $\sqrt{s} = 1.96$ TeV”. In: *Phys. Lett. B* 695 (2011), p. 88. ISSN: 0370-2693. DOI: 10.1016/j.physletb.2010.10.059. arXiv:1008.2023 [hep-ex].

[42] T. Aaltonen et al. “Search for high mass resonances decaying to muon pairs in $\sqrt{s} = 1.96$ TeV $\mathrm{p\bar{p}}$ collisions”. In: *Phys. Rev. Lett.* 106 (2011), p. 121801. DOI: 10.1103/PhysRevLett.106.121801. arXiv:1101.4578 [hep-ex].

[43] T. Aaltonen et al. “Search for new dielectron resonances and Randall–Sundrum gravitons at the Collider Detector at Fermilab”. In: *Phys. Rev. Lett.* 107 (2011), p. 051801. DOI: 10.1103/PhysRevLett.107.051801. arXiv:1103.4650 [hep-ex].

[44] Vardan Khachatryan et al. “Search for anomalous Wtb couplings and flavour-changing neutral currents in t-channel single top quark production in pp collisions at $\sqrt{s} = 7$ and 8 TeV”. In: *JHEP* 02 (2017), p. 028. DOI: 10.1007/JHEP02(2017)028. arXiv:1610.03545 [hep-ex].

[45] Vardan Khachatryan et al. “Measurement of the W boson helicity in events with a single reconstructed top quark in pp collisions at $\sqrt{s} = 8$ TeV”. In: *JHEP* 01 (2015), p. 053. DOI: 10.1007/JHEP01(2015)053. arXiv:1410.1154 [hep-ex].

[46] Morad Aaboud et al. “Probing the Wtb vertex structure in t-channel single-top-quark production and decay in pp collisions at $\sqrt{\mathrm{s}} = 8$ TeV with the ATLAS detector”. In: *JHEP* 04 (2017), p. 124. DOI: 10.1007/JHEP04(2017)124. arXiv:1702.08309 [hep-ex].

[47] Morad Aaboud et al. “Measurement of the W boson polarisation in $t\bar{t}$ events from pp collisions at $\sqrt{s} = 8$ TeV in the lepton+jets channel with ATLAS”. In: *Eur. Phys. J.* C77.4 (2017), p. 264. DOI: 10.1140/epjc/s10052-017-4819-4. arXiv:1612.02577 [hep-ex].

[48] Victor Mukhamedovich Abazov et al. “Combination of searches for anomalous top quark couplings with 5.4 fb^{-1} of $p\bar{p}$ collisions”. In: *Phys. Lett.* B713 (2012), pp. 165–171. DOI: 10.1016/j.physletb.2012.05.048. arXiv:1204.2332 [hep-ex].

[49] Georges Aad et al. “Search for single top-quark production via flavour-changing neutral currents at 8 TeV with the ATLAS detector”. In: *Eur. Phys. J. C* 76 (2016), p. 55. DOI: 10.1140/epjc/s10052-016-3876-4. arXiv:1509.00294 [hep-ex].

[50] Victor Mukhamedovich Abazov et al. “Search for flavor changing neutral currents via quark-gluon couplings in single top quark production using 2.3 fb^{-1} of $p\bar{p}$ collisions”. In: *Phys. Lett.* B693 (2010), pp. 81–87. DOI: 10.1016/j.physletb.2010.08.011. arXiv:1006.3575 [hep-ex].

[51] T. Aaltonen et al. “Search for top-quark production via flavor-changing neutral currents in W+1 jet events at CDF”. In: *Phys. Rev. Lett.* 102 (2009), p. 151801. DOI: 10.1103/PhysRevLett.102.151801. arXiv:0812.3400 [hep-ex].

[52] The CMS Collaboration. “Search for new physics via top quark production in dilepton final state at 13 TeV”. In: *CMS Physics Analysis Summaries* CMS-PAS-TOP-17-020 (2018).

[53] Particle Data Group. “Review of Particle Physics”. In: *Chin. Phys.* C40.10 (2016), p. 100001. DOI: 10.1088/1674-1137/40/10/100001.

[54] Alan D. Martin Francis Halzen. “QUARKS AND LEPTONS: An introductory Course in Modern Particle Physics”. In: JOHN WILEY and SONS (1984).

[55] Emmy Noether. “Invariant variation problems”. In: *Transport Theory and Statistical Physics* 1.3 (1971), pp. 186–207. DOI: 10.1080/00411457108231446. eprint: https://doi.org/10.1080/00411457108231446. URL: https://doi.org/10.1080/00411457108231446.

[56] F. Englert and R. Brout. “Broken Symmetry and the Mass of Gauge Vector Mesons”. In: *Phys. Rev. Lett.* 13 (9 1964), pp. 321–323. DOI: 10.1103/PhysRevLett.13.321. URL: https://link.aps.org/doi/10.1103/PhysRevLett.13.321.

[57] P.W. Higgs. “Broken symmetries, massless particles and gauge fields”. In: *Physics Letters* 12.2 (1964), pp. 132 –133. ISSN: 0031-9163. DOI: https://doi.org/10.1016/0031-9163(64)91136-9. URL: http://www.sciencedirect.com/science/article/pii/0031916364911369.

[58] Peter W. Higgs. “Broken Symmetries and the Masses of Gauge Bosons”. In: *Phys. Rev. Lett.* 13 (16 1964), pp. 508–509. DOI: 10.1103/PhysRevLett.13.508. URL: https://link.aps.org/doi/10.1103/PhysRevLett.13.508.

[59] Steven Weinberg. “A Model of Leptons”. In: *Phys. Rev. Lett.* 19 (21 1967), pp. 1264–1266. DOI: 10.1103/PhysRevLett.19.1264. URL: https://link.aps.org/doi/10.1103/PhysRevLett.19.1264.

[60] Abdus Salam and J. C. Ward. “Weak and electromagnetic interactions”. In: *Il Nuovo Cimento (1955-1965)* 11.4 (1959), pp. 568–577. ISSN: 1827-6121. DOI: 10.1007/BF02726525. URL: https://doi.org/10.1007/BF02726525.

[61] Sheldon L. Glashow. “The renormalizability of vector meson interactions”. In: *Nuclear Physics* 10 (1959), pp. 107 –117. ISSN: 0029-5582. DOI: https://doi.org/10.1016/0029-5582(59)90196-8. URL: http://www.sciencedirect.com/science/article/pii/0029558259901968.

[62] B.R. WEBBER R.K. ELLIS W.J. STIRLING. “QCD and Collider Physics”. In: (1996).

[63] CODATA Value: Fermi coupling constant. “The NIST Reference on Constants, Units, and Uncertainty”. In: *US National Institute of Standards and Technology* (June 2015. Retrieved 2016-10-31).

[64] The CMS collaboration. “Measurement of the Drell-Yan cross section in pp collisions at $\sqrt{s} = 7$ TeV”. In: *Journal of High Energy Physics* 2011.10 (2011), p. 7. ISSN: 1029-8479. DOI: 10.1007/JHEP10(2011)007. URL: https://doi.org/10.1007/JHEP10(2011)007.

[65] Dimitri Bourilkov. “Exploring the LHC Landscape with Dileptons”. In: *arXiv* 1609.08994 (2017).

[66] M. Peskin. “Beyond the Standard Model”. In: *Lectures notes of the 1996 European School of High-Energy Physics* (Carry-le-Rouet, France, 1996).

[67] K.A. Olive and Particle Data Group. “Review of Particle Physics”. In: *Chinese Physics C* 38.9 (2014), p. 090001. URL: http://stacks.iop.org/1674-1137/38/i=9/a=090001.

[68] Adam G. Riess et al. “Observational evidence from supernovae for an accelerating universe and a cosmological constant”. In: *Astron. J.* 116 (1998), pp. 1009–1038. DOI: 10.1086/300499. arXiv:astro-ph/9805201 [astro-ph].

[69] S. Perlmutter et al. “Measurements of Omega and Lambda from 42 high redshift supernovae”. In: *Astrophys. J.* 517 (1999), pp. 565–586. DOI: 10.1086/307221. arXiv:astro-ph/9812133 [astro-ph].

[70] A D. SAKHAROV. “Violation of CP invariance, 小asymmetry, and baryon asymmetry of the universe”. In: vol. 5. Nov. 1998, pp. 84–87. ISBN: 978-981-02-3606-9. DOI: 10.1142/9789812815941_0013.

[71] Nicola Cabibbo. “Unitary Symmetry and Leptonic Decays”. In: *Phys. Rev. Lett.* 10 (12 1963), pp. 531–533. DOI: 10.1103/PhysRevLett.10.531. URL: https://link.aps.org/doi/10.1103/PhysRevLett.10.531.

[72] Makoto Kobayashi and Toshihide Maskawa. “CP-Violation in the Renormalizable Theory of Weak Interaction”. In: *Progress of Theoretical Physics* 49.2 (Feb. 1973), pp. 652–657. ISSN: 0033-068X. DOI: 10.1143/PTP.49.652. eprint: http://oup.prod.sis.lan/ptp/article-pdf/49/2/652/5257692/49-2-652.pdf. URL: https://doi.org/10.1143/PTP.49.652.

[73] T. Schäfer and E. V. Shuryak. “Instantons in QCD”. In: *Rev. Mod. Phys.* 70 (2 1998), pp. 323–425. DOI: 10.1103/RevModPhys.70.323. URL: https://link.aps.org/doi/10.1103/RevModPhys.70.323.

[74] The CMS and ATLAS Collobarations. “Measurements of the Higgs boson production and decay rates and constraints on its couplings from a combined ATLAS and CMS analysis of the LHC pp collision data at $\sqrt{s} = 7$ and 8 TeV”. In: *JHEP* 08 (2016), p. 045. DOI: 10.1007/JHEP08(2016)045. arXiv:1606.02266 [hep-ex].

[75] Stephen P. Martin. “A Supersymmetry primer”. In: *Adv. Ser. Direct. High Energy Phys.18,1* (1997). DOI: 10.1142/9789812839657_0001, 10.1142/9789814307505_0001. arXiv:hep-ph/9709356 [hep-ph].

[76] R. Barbier et al. “R-Parity-violating supersymmetry”. In: *Physics Reports* 420.1 (2005), pp. 1 – 195. ISSN: 0370-1573. DOI: https://doi.org/10.1016/j.physrep.2005.08.006. URL: http://www.sciencedirect.com/science/article/pii/S0370157305003327.

[77] H. Georgi and S. Glashow. “Unity of All Elementary Particle Forces”. In: *Phys. Rev. Lett.* 32 (1974), p. 438. DOI: 10.1103/PhysRevLett.32.438.

[78] R. C. King, L. Dehuai, and B. G. Wybourne. “Symmetrized Powers of Rotation Group Representations”. In: *J. Phys.* A14 (1981), pp. 2509–2538. DOI: 10.1088/0305-4470/14/10/009.

[79] Edward Witten. “Symmetry Breaking Patterns in Superstring Models”. In: *Nucl. Phys.* B258 (1985), p. 75. DOI: 10.1016/0550-3213(85)90603-0.

[80] Edward Witten. “Symmetry breaking patterns in superstring models”. In: *Nuclear Physics B* 258 (1985), pp. 75 –100. ISSN: 0550-3213. DOI: https://doi.org/10.1016/0550-3213(85)90603-0. URL: http://www.sciencedirect.com/science/article/pii/0550321385906030.

[81] John H. Schwarz. “Introduction to superstring theory”. In: *NATO Sci. Ser. C* 566 (2001), pp. 143–187. DOI: 10.1007/978-94-010-0522-7_4. arXiv:0008017 [hep-ex].

[82] Cen Zhang and Scott Willenbrock. “Effective-Field-Theory Approach to Top-Quark Production and Decay”. In: *Phys. Rev.* D83 (2011), p. 034006. DOI: 10.1103/PhysRevD.83.034006. arXiv:1008.3869 [hep-ph].

[83] Gauthier Durieux, Fabio Maltoni, and Cen Zhang. “Global approach to top-quark flavor-changing interactions”. In: *Phys. Rev. D* 91 (2015), p. 074017. DOI: 10.1103/PhysRevD.91.074017. arXiv:1412.7166 [hep-ph].

[84] B. Grzadkowski et al. “Dimension-Six Terms in the Standard Model Lagrangian”. In: *JHEP* 10 (2010), p. 085. DOI: 10.1007/JHEP10(2010)085. arXiv:1008.4884 [hep-ph].

[85] Peter L. Cho and Elizabeth H. Simmons. “Searching for G3 in $\mathrm{t\bar{t}}$ production”. In: *Phys. Rev. D* 51 (1995), p. 2360. DOI: 10.1103/PhysRevD.51.2360. arXiv:hep-ph/9408206 [hep-ph].

[86] CMS Collaboration. “Search for Anomalous Top Chromomagnetic Dipole Moments from angular distributions in $t\bar{t}$ Dileptonic events at $\sqrt{s} = 7$ TeV with the CMS detector”. In: *CMS-PAS-TOP-14-005* (2014).